CHAPTER 2
MEASUREMENT METHODS FOR SOUND AND VIBRATION PERFORMANCES, INCLUDING LOW FREQUENCIES

COST Action FP0702

Net-Acoustics for Timber based Lightweight Buildings and Elements

Working Group 2: Measurement methods for sound and vibration performances

CONTENTS

This chapter presents six documents, written by different COST FP0702 member institutes and focused on general methods for measuring the main sound or vibration quantities, relevant for evaluating and predicting building performances.

Concerning *sound performances*, low-frequency airborne and impact sound insulation is especially important in lightweight buildings because of the low levels of sound insulation in the low-frequency range. Existing measurement methods show poor repeatability, reproducibility and relevance to room occupants in the low-frequency range. Improved procedures are proposed in the first two papers presented: the first paper proposes an improved procedure for measuring airborne sound insulation between rooms, from work performed at the University of Liverpool UK; a second paper proposes the use of sound intensity for measuring direct impact sound, from work performed at the University of Applied Sciences of Rosenheim, Germany.

Another difficulty appears in predicting acoustic performances of lightweight building, where, as explained in chapter 1 of this e-book, new (or modified) quantities are required. The third paper presented proposes methods for estimating two key quantities: the radiation efficiency of building elements and the velocity level difference of junctions between elements. Examples of results are given from work performed at CSTB France.

Concerning *vibration performances* of floors with respect to walking induced vibration, several key parameters are identified in the paper on vibration prediction presented in chapter 1: static floor deflection, floor fundamental frequency, unit floor response and single step floor response. Three papers related to these quantities and focusing on measurement methods are presented in chapter 2: the first paper presents a procedure for measuring floor deflection as used at SINTEF Buildings & Infrastructures, Norway; a second paper gives methods and examples on how to measure unit floor response (and goes even further through modal analysis, thus identifying resonant frequencies and mode shapes) and damping, from work performed at the University of Science and Technology of Trondheim, Norway; a third paper focuses on single step floor response, applied to both "own" floor and neighboring floor (through junctions), from work performed at TNO, The Netherlands.

1 - NEW PROPOSAL FOR FIELD SOUND INSULATION MEASUREMENTS IN THE LOW-FREQUENCY RANGE

Document written by Carl Hopkins
Acoustics Research Unit, School of Architecture, University of Liverpool, UK

Low-frequency airborne and impact sound insulation is important in all buildings, but especially lightweight buildings. The reason for this is that walls or floors with a low mass per unit area typically have low levels of sound insulation in the low-frequency range. Standard procedures for field measurements of sound insulation between rooms are currently described in the ISO 140 series of International Standards. However, they are intended for use in rooms with sound fields that approximate diffuse fields. In practice, many dwellings contain rooms with volumes less than 25m^3, where the absence of a diffuse sound field at low-frequencies combined with the sampling of sound pressure in the central zone of a room makes measurements less reliable, and less relevant to building occupants. On the basis that sound insulation in the low-frequency range (particularly below 100Hz) is of importance in all buildings, but especially timber frame buildings, this COST FP0702 project provided the impetus to draw on recent research [1] to define new procedural changes that would improve the reliability and relevance of field sound insulation measurements. These procedural changes were subsequently used in a proposal to revise four International Standards on field sound insulation testing (ISO 140 Parts 4, 5, 7 and 14) at the ISO TC43 SC2 plenary session in Korea (November, 2009). This proposal was accepted and Carl Hopkins became the convenor of the work packages to write these new Standards. The first new International Standard, ISO/DIS 16283-1, has been written on the field measurement of airborne sound insulation and was circulated to all countries as a draft for comment in Spring 2012 [2].

Two measurement procedures are described in ISO/DIS 16283-1 to measure the sound pressure level, the reverberation time and the background noise; a default procedure and an additional low-frequency procedure. The default procedure for all frequencies is to obtain the energy-average sound pressure level using a fixed microphone or a manually-held microphone moved from one position to another, an array of fixed microphones, a mechanized continuously-moving microphone or a manually-scanned microphone. These measurements are taken in the central zone of a room at positions away from the room boundaries. A new low-frequency procedure is introduced for the 50, 63, 80 Hz one-third octave bands in the source and/or receiving room when its volume is smaller than 25 m^3 (calculated to the nearest cubic metre). This procedure is carried out in addition to the default procedure and requires additional measurements of the sound pressure level in the corners of the source and/or receiving room using either a fixed microphone or a manually-held microphone. For the low-frequency procedure a fixed microphone is positioned in room corners at a distance of 0.3 m to 0.4 m from each room boundary that forms the corner – see Figure 1.

Figure 1. Fixed microphone in a room corner.

The low-frequency energy-average sound pressure level in the 50 Hz, 63 Hz and 80 Hz bands is calculated by combining the spatial-average sound pressure level, L, from the default procedure in the central zone of the room with L_{Corner} from the low-frequency procedure using

$$L_{\text{LF}} = 10\lg\left[\frac{10^{0,1L_{\text{Corner}}} + (2\cdot 10^{0,1L})}{3}\right]$$

An example illustrating the improvement in the repeatability of measurements is shown in Figure 2 from sound pressure level measurements in a 29m^3 source room and an 18m^3 receiving room. For measurements in the central zone of the room it is common to use a set of five stationary microphone positions; hence each different set of five positions will contribute to the uncertainty in the spatial average value. For the default procedure, Figure 2(a) shows the results for many different sets of five positions in terms of the mean and 95% confidence intervals that have been normalized to the average of all possible positions in the central zone of the room. The uncertainty is large below 100Hz where the 95% confidence intervals span a range of 4 to 7 dB. This can be compared with Figure 2(b) which uses the low-frequency procedure and shows that the mean error is only 0dB to 1dB when using the low-frequency procedure to estimate the average sound pressure level over the entire room volume (i.e. including positions at the walls and corners). More importantly, the 95% confidence intervals for the low-frequency procedure are typically less than 2dB; hence they are similar to the uncertainty of the default procedure in the central zone for different sets of stationary microphone positions between 100 and 500 Hz. The low-frequency procedure can therefore be used in small rooms which have large spatial variations in the sound pressure level to improve the repeatability, reproducibility and relevance to room occupants.

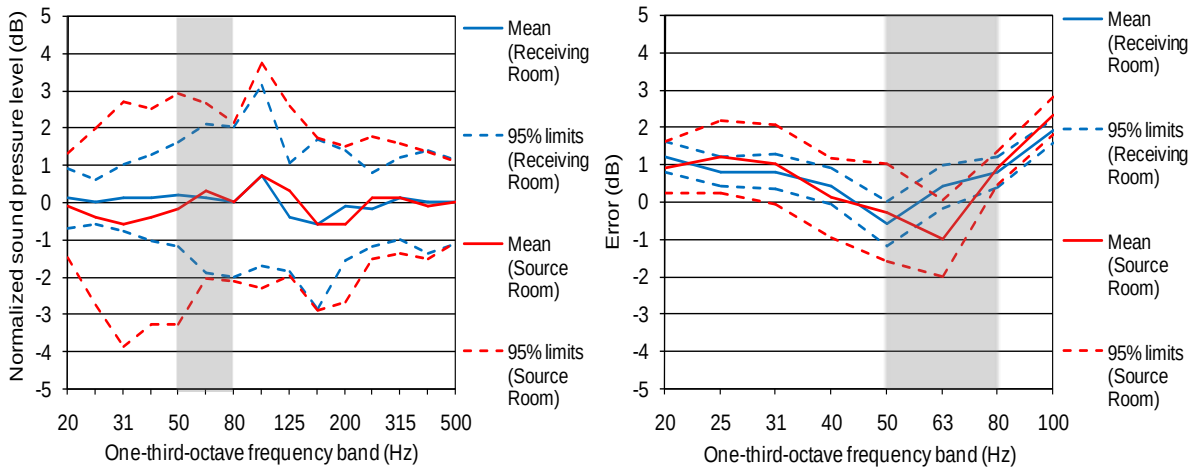

(a) (b)

Figure 2. (a) default procedure in the central zone of a room (b) low-frequency procedure using corner measurements. NB Grey shaded areas highlight the 50, 63 and 80 Hz one-third octave bands.

In timber or steel frame buildings with gypsum or timber board linings the reverberation times in the 50 Hz, 63 Hz and 80 Hz bands can be sufficiently short that the decay curve is affected by the decay time of the one-third octave band filters in the analyser. Typically they are 0.3s < T < 0.8s for room volumes of 20 to 60m^3. Problems can be avoided by using a 63 Hz octave band filter due to its wider bandwidth which allows the measurement of shorter reverberation times. In addition, in small rooms there are relatively few room modes that determine the decay curve in the 50 Hz, 63 Hz and 80 Hz bands. Hence the use of 20 dB or 30 dB evaluation ranges on the decay curves from one-third octave bands are prone to error because single-slope decay curves usually only occur when there are many modes in each frequency band. This issue can partly be resolved through use of the 63 Hz octave band filter. The solution proposed in ISO/DIS 16283-1 is to define a default procedure that shall be used in the receiving room for all reverberation time measurements, and a low-frequency procedure that shall be used when the receiving room volume is smaller than 25m^3. The low-frequency procedure requires that the reverberation time is measured in the 63 Hz octave band instead of the 50 Hz, 63 Hz, 80 Hz one-third octave bands and that this single measured value is used to represent the 50 Hz, 63 Hz and 80 Hz bands in the calculation of D_{nT} and/or R'.

Approximately 250 individual reverberation time measurements using forward filter analysis with interrupted noise in unfurnished timber and steel frame buildings were used to assess the efficacy of this approach [1]. A summary is shown in Table 1.

One-third-octave band centre frequency (Hz)	% satisfying *BT* > 8 criterion	
	Using individual decay curves	Using ensemble average decay curves
50	37 %	33 %
63	48 %	57 %
80	87 %	86 %

Octave band centre frequency (Hz)	% satisfying *BT* > 8 criterion	
	Using individual decay curves	Using ensemble average decay curves
63	98.8 %	100 %

Table 1. Percentage of reverberation times satisfying the BT>8 criterion in timber and steel frame buildings when using one-third octave bands compared to octave bands.

In the near future, the same low-frequency procedures will also be introduced for impact sound insulation and facade sound insulation in the next two parts of the Standard that will be drafted in 2012/2013.

1.1 - References

[1] C. Hopkins and P. Turner. Field measurement of airborne sound insulation between rooms with non-diffuse sound fields at low frequencies. Applied Acoustics 66 (2005) 1339–1382.

[2] ISO/DIS 16283-1:2012. Acoustics - Field measurement of sound insulation in buildings and of building elements - Part 1: Airborne sound insulation.

2 - LF IMPACT SOUND LEVEL USING INTENSITY,

Document written by U. Schanda and F. Schöpfer

University of Applied Sciences Rosenheim, Germany

2.1 - Introduction

In a recently completed R&D project at the University of Applied Sciences Rosenheim a practical prediction tool based on EN 12354 for sound transmission of timber joist floors in heavy-weight buidings was developed and validated [1]. Usually the sound transmission of timber joist floors before remedial actions is dominated by direct sound transmission, whereas flanking transmission becomes more important after remedial actions. For measurements of airborne as well as impact sound insulation, timber joist floor constructions usually found in old buildings have been rebuilt in the laboratory and were measured according to ISO 140. Here, special consideration was given to the frequency range below 100 Hz. After that, the tested floor constructions were acoustically improved by various common remedial actions and measured again. Also, flanking sound transmission was determined in the laboratory by means of measurements using brick walls with different mass per unit area. In order to validate the prediction tool, field measurements were conducted as well. In these cases, the direct sound transmission was obtained using the intensity method according to the procedures described in ISO 15186. However, for impact sound transmission there is no measurement procedure found in the literature so far. Therefore a measurement survey has been performed on a concrete floor as well as on a timber joist floor similar to model 1 given in appendix B of ISO 140 – 11 and equipped with a floating screed. The results of this laboratory survey comparing impact sound insulation according to ISO 140 with intensity based impact sound insulation are presented. Another reason for detailed investigation of intensity based sound insulation measurements is due to the ongoing discussion about measuring sound insulation at low frequencies. Measurements of sound level as well as reverberation time at low frequencies are still problematic and are usually affected by various inaccuracies. The intensity method is expected to cope with these shortcomings.

2.2 - Basic equations

The following notation is based on the German version of the standard ISO 140 (ISO 10140 resp.) and the standard ISO 15186.

The normalized impact sound level L_n is given by the impact sound level L_i as

$$L_n = L_i + 10 \cdot \log\left(\frac{A}{10\,\mathrm{m}^2}\right).$$

Assuming that the impact sound level originates from a diffuse sound field, it can be written in terms of the sound power level of the source, which in our case is the floor, as

$$L_i = L_W + 10 \cdot \log\left(\frac{4 \cdot \mathrm{m}^2}{A}\right).$$

The sound power level L_W of the source can be written in terms of the normal sound intensity level L_{In} as

$$L_W = L_{In} + 10 \cdot \log\left(\frac{S}{\mathrm{m}^2}\right).$$

Therefore the normalized impact sound (intensity) $L_{n,I}$ level is given by

$$L_{n,I} = L_{In} + 10 \cdot \log\left(\frac{S}{\mathrm{m}^2}\right) - 4\,\mathrm{dB}.$$

In order to compare this normalized impact sound (intensity) level with the normalized impact sound level from measurements according to ISO 140- 4, it is necessary to account for sound pressure enhancement near the surface similar to the standard ISO 15186. Therefore a modified normalized impact sound intensity level $L_{n,I,\mathrm{M}}$ is introduced. This modified normalized impact sound (intensity) level $L_{n,I,\mathrm{M}}$ can be written as

$$L_{n,I,\mathrm{M}} = L_{n,I} - K_C$$

with K_C as the Waterhouse correction [2] calculated according to Uosukainen [3] as

$$K_C = 10 \cdot \log\left(1 + \frac{S_b \cdot \lambda}{8 \cdot V} + \frac{L \cdot \lambda^2}{32 \cdot \pi \cdot V}\right).$$

The additional term in the argument of the logarithm given by Uosukainen increases the adaption term of ISO 15186 of less than 1 dB at 50 Hz for any common room size.

2.3 - Laboratory measurements

2.3.1 - Measurement conditions

2.3.1.1 - ***Intensity probe and measurement procedure***

For the measurements an intensity pp-probe of type Norsonic 240 together with a Norsonic Real Time Analyser 840 was used. Besides the mandatory calibration procedure additional verifications of the measurement system were carried out using identical intensity

equipment and exchange intensity probes and analysers. For the measurements the probe was used with a 50 mm spacer. Therefore the frequency range possible for data evaluation was restricted from 40 Hz to 1600 Hz. Due to ageing effects the intensity probe used did not fulfill the criteria of class I measurement accuracy below 200 Hz. The residual PI-index obtained decreased from 18 dB at 200 Hz to 10 dB at 50 Hz (class I measurement accuracy requires 19 dB at 200 Hz and 12 dB at 50 Hz).

The measurements were performed using the scanning procedure according to ISO 15186. The distance of the intensity probe to the ceiling was 0,2 m, the scanning speed was 0,2 m/s, the distance of the scanning paths was 0,2 m.

2.3.1.2 - ***Conditioning of the receiving room***

The bottom of the receiving room was equipped with sound absorbing material. In figure 1 the arrangement is shown. The sound absorption coefficient of this arrangement for normal incidence was measured in a Kundt's tube. It is greater than 0,8 in the frequency range above 50 Hz. At a vertical height of approx. 0,8 m a metal grid was positioned in order to provide an operating platform.

Figure 1: sound absorption layer opposite the measurement surface

2.3.1.3 - ***Measurement area***

In order to minimize the measurement effort an investigation on smaller measurement subareas was made and compared to results of the whole ceiling. This survey was carried out on the above mentioned timber joist floor. The volume of the receiving room was approx. 50 m^3. The standard tapping machine was placed at six positions on the floor as indicated in figure 2. The ceiling area was divided into six subareas, also shown in figure 2.

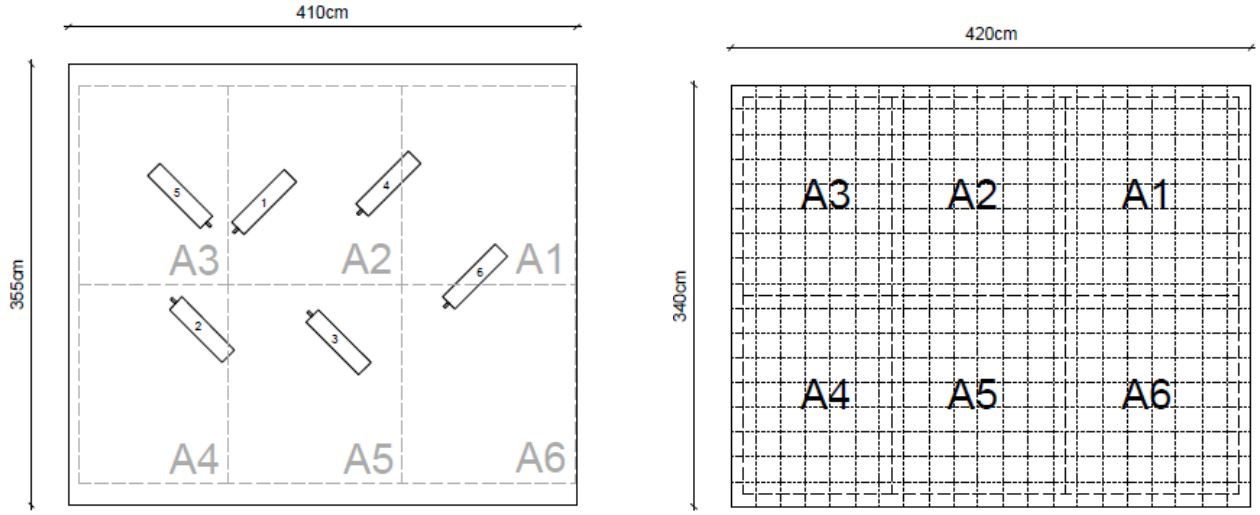

Figure 2: positions of the standard tapping machine and partition of the ceiling area into six subareas

In this laboratory survey an intensity measurement of subarea A7 only was carried out as well (see figure 3).

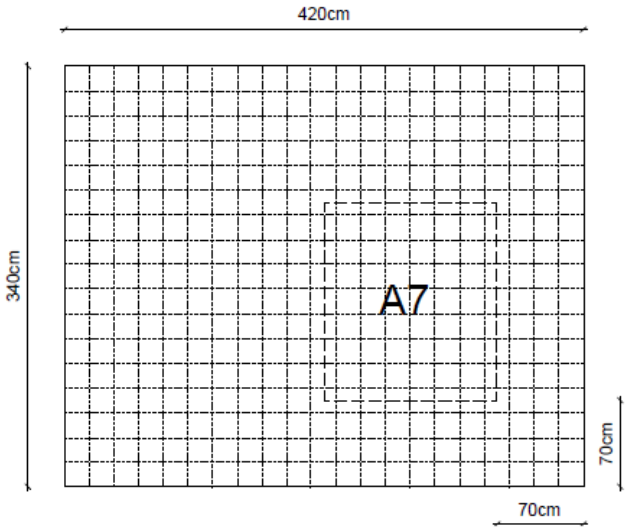

Figure 3: Single measurement subarea used for reduced measurement procedure

Figure 4 shows a comparison of the arithmetic mean intensity level of the six subareas A1 - A6 and the single value of subarea A7. At frequencies below 125 Hz differences of up to 2.5 dB occur. In fact a dependency of the distance of the tapping machine to the

measurement subarea was observed, especially with respect to the PI-Index of the measurements. The bigger the distance of the tapping machine to the measurement subarea considered, the higher the PI-Index of the measurement. The difference may amount to 8 dB in the PI-Index.

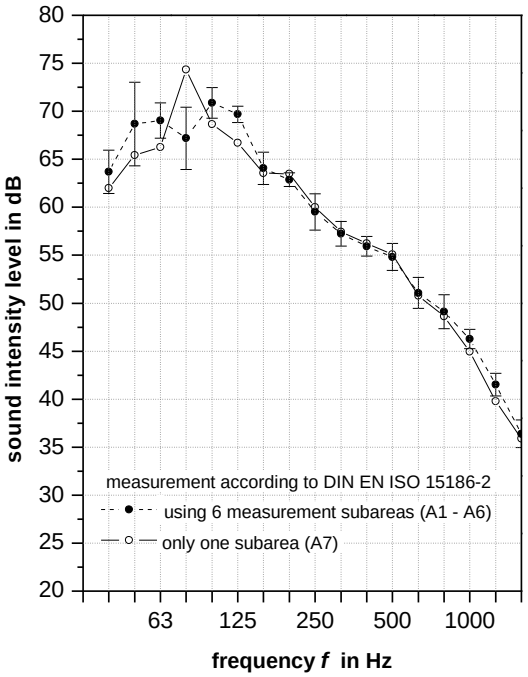

figure 4: Comparison of the sound intensity level, using the whole measurement surface (mean of subareas A1- A6, see figure 2) and the sound intensity level from subarea A7 (see figure 3). Uncertainty bars indicate the standard deviation of the measurements of the six subareas.

2.3.2 - Comparison of ISO 140 and ISO 15186 measurements

In order to compare measurement results in terms of impact sound level and sound insulation, measurements according to ISO 140 and ISO 15186 have been performed in a test facility without flanking transmission. The separating element for these test was a concrete floor of 14 cm thickness without any flooring. The volume of the receiving room was 69 m^3.

In figure 5 comparisons are shown. On the right hand side the figure shows the measurements of L_n and $L_{n,I,M}$ respectively, with the difference of these curves given at the top. Although the Waterhouse correction according to chapter 2 was applied, the discrepancy between the two measurement methods at low frequencies is evident. Similar result were obtained for the difference of R and $R_{I,M}$, shown on the left hand side of figure 5.

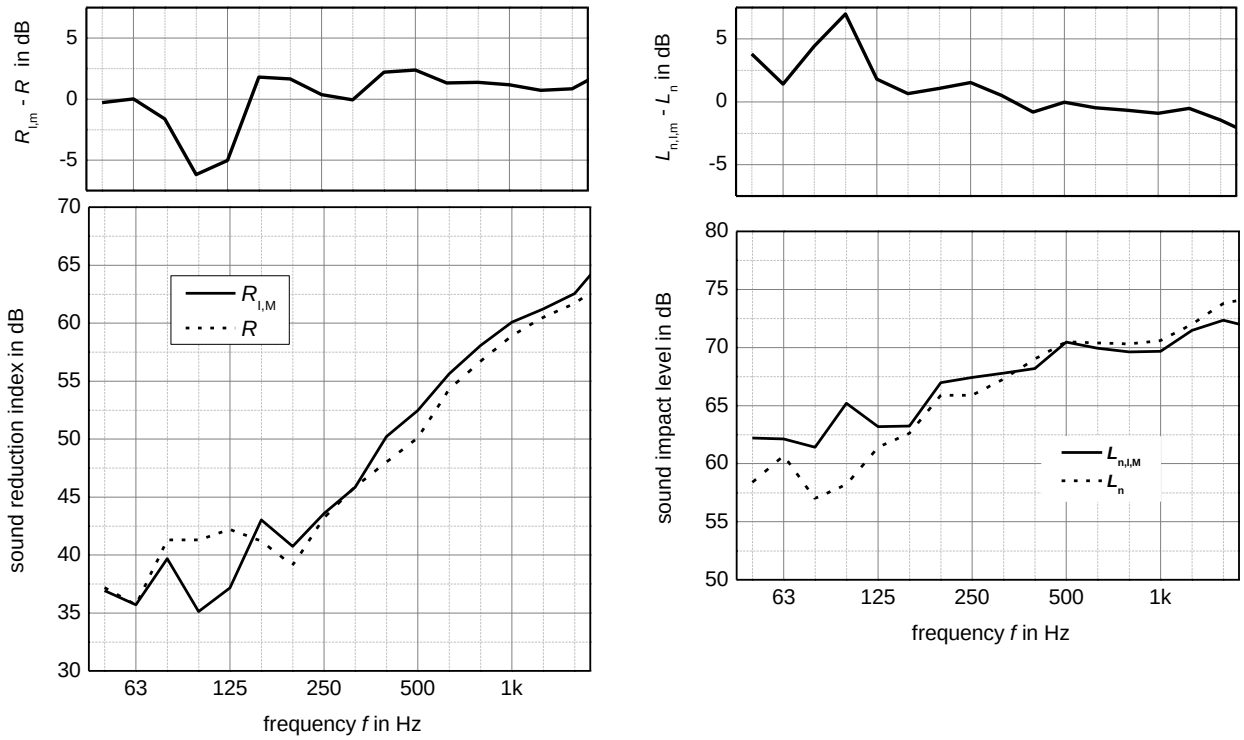

Figure 5: Comparison of the modified intensity impact sound level $L_{n,I,M}$ with the impact sound level L_n at the right hand side and the modified intensity sound reduction index $R_{I,M}$ according to ISO15186 with the sound reduction index R according to ISO 140 at the left hand side. At low frequencies a deviation is observable, which occured in both measurements.

The observed difference might be caused by uncertainties in the reverberation time, which is required for calculation of L_n. Especially at low frequencies, where room resonances may occur, exact determination of the reverberation time is difficult. However, in this measurement the reverberation time of the receiving room was quite short in low frequencies due to additional drywalls in front of the heavy-weight flanking walls and therefore had rather smooth characteristics (see figure 6). Also shown in figure 6 is the corner sound pressure level which indicates resonances at frequencies which correspond to half a wavelength in room dimension. Therefore more investigation is required in order do identify and understand the discrepancies between the different measurement methods in the low frequency region, shown in figure 5. Nevertheless the fact that the same discrepancy occur in both impact sound level measurements and sound reduction measurements indicate that measurement of impact sound level using sound intensity method is possible even at low frequencies.

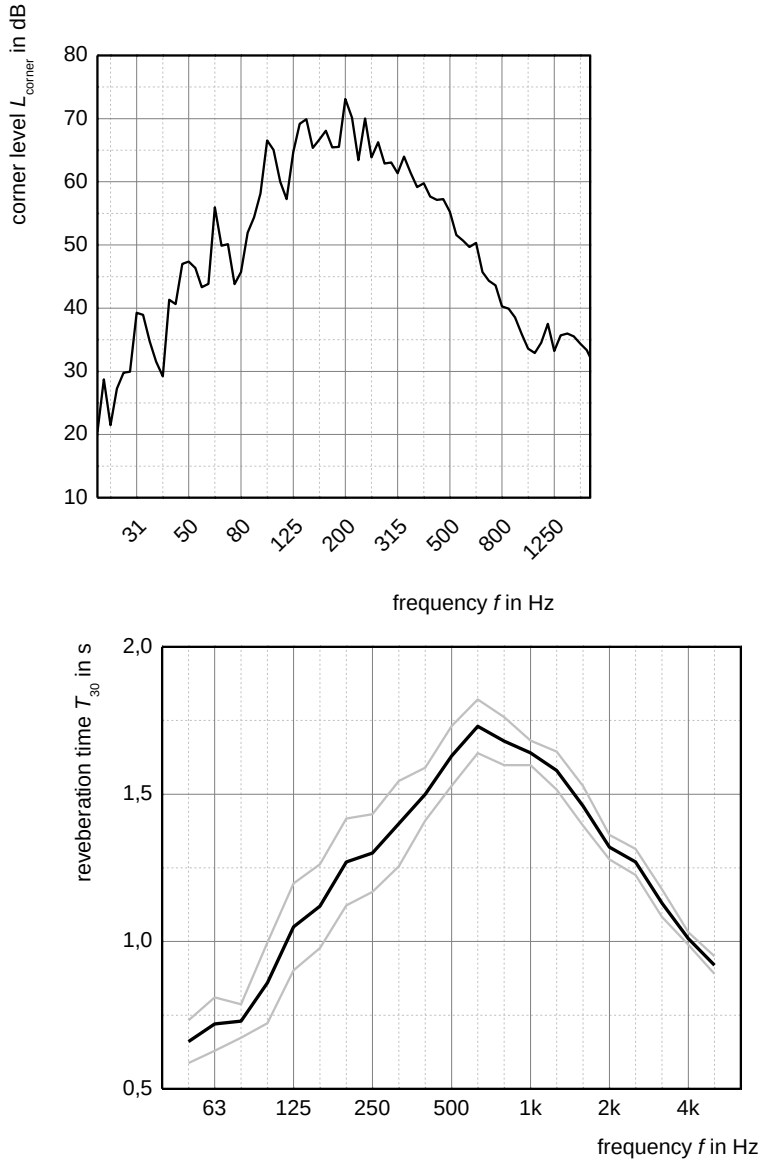

Figure 6: receiving room reverberation time and corner sound pressure level

2.4 - Field measurements

In the course of the mentioned R&D project field tests on various timber joist floors were carried out by measuring the sound insulation of the direct path using the intensity method. The contribution of the flanking paths (solid, heavy-weight walls) was obtained by measuring the surface velocity and assuming a unit radiation efficiency. The energetic sum of the individual transmission paths then yields the total sound reduction index R'_{sum}. Additionally the sound reduction index R' was directly measured according to ISO 140. The difference between both approaches is shown on the left hand side of figure 7. Results of the individual measurements are provided with the mean indicated by a bold line. The graph on the right hand side of figure 7 shows the difference of the impact sound level respectively. Again, the measurement of the direct path contributing to the impact sound level was carried out using the intensity approach described above.

Both graphs reveal a discrepancy in the low frequency range. This deviation is systematic in that the measured intensity sound levels are obviously higher compared to values obtained according to ISO 140.

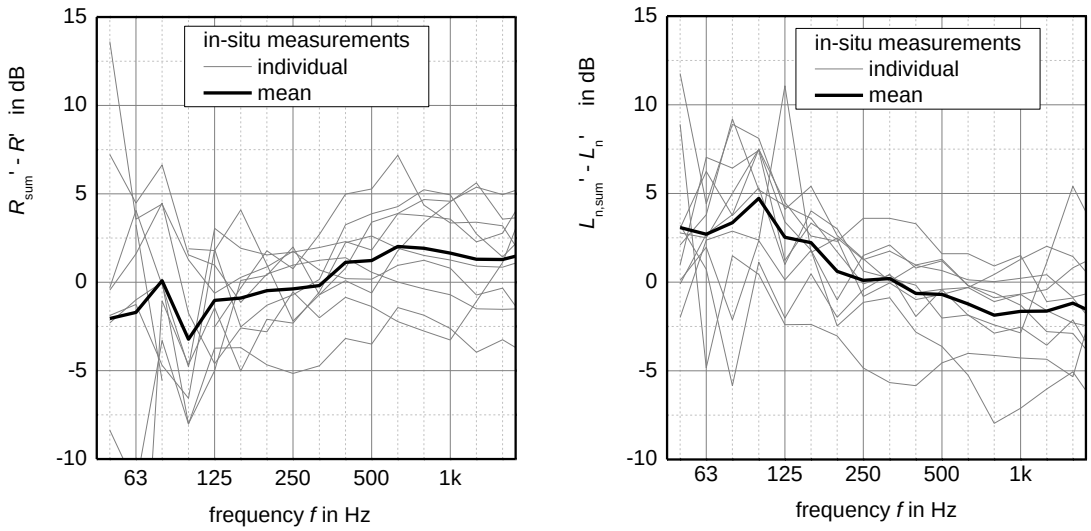

Figure 7: Comparison of in-situ measurements of airborne and impact sound insulation according to ISO 140 with results obtained by measuring the direct path of the sound transmission with intensity and the flanking paths with accelerometer and combining the contributions to a total sound reduction R'_{sum} and $L'_{n,sum,}$ respectively.

2.5 - Conclusion

Results of laboratory and field surveys indicate that measurements of impact sound level using the intensity method combined with the equations given in chapter 2 is feasible and yield reasonable results even in the low frequency range. The advantage of this measurement approach is the independency on the rooms reverberation time and sound level which might vary, especially at low frequencies. The disadvantage is the large instrumental and operating expense. The reduction of measurement time in using only one subarea instead of scanning the whole ceiling seems to be possible if less accuracy is acceptable. However, this needs to be verified systematically, especially for inhomogeneous constructions like timber joist floors. A systematic deviation compared to conventional measurement results according to ISO 140 was found in the low frequency range, despite the application of the Waterhouse correction. These results confirm the findings of others published before [4], [5], [6], [7], [8] and need further investigation.

2.6 - References

[1] RABOLD A., MAYR A., SCHÖPFER F., BACHER S., SCHANDA U.: Timber joist floors in heavy-weight buildings – engineering tools for remedial measures improving sound transmission loss; submitted to Bauphysik, 2012, in German

[2] WATERHOUSE R.V.: Interference patterns in reverberant sound fields; The Journal of the acoustical society of America (1955), 247-258

[3] UOSUKAINEN S.: On the use of the Waterhouse Correction; Journal of sound and Vibration (1995), 223-230

[4] JACOBSEN F., DING H.: Observations on the systematic deviations between two methods of measuring sound transmission loss; Building Acoustics, Vol. 3, (1997), 1-11

[5] PEDERSON D.B., ROLAND J., RAABE G., MAYSENHÖLDER W.: Measurement of the low-frequency sound insulation of building components; Acoustica 86, (2000), 495-505

[6] VORLÄNDER M., WARNCOCK A.C.C.: *Inter-Laboratory Comparison of low frequency sound transmission: conventional and intensity measurements.* Proceedings of inter-noise 93, Leuven, Belgium (1993), 933-936

[7] MACHIMBARRENA M., JACOBSEN F.: *Is there a systematic disagreement between intensity-based and pressure-based sound transmission loss measurements?* Building Acoustics, Vol. 6 (1999), 101-111

[8] HALLIWELL R.E., WARNCOCK A.C.C.: *Sound transmission loss: Comparison of conventional techniques with sound intensity technique*, Journal of Acoustical Society of America, Vol. 77 ,(1985), 2094-2103

3 - METHODS FOR MEASURING RADIATION EFFICIENCY AND JUNCTION VIBRATION LEVEL DIFFERENCE

Document written by Michel Villot and Catherine Guigou-Carter
Center for Building Science and Technology, CSTB-DAE, Grenoble France

The proposal for prediction of acoustic performances of lightweight buildings presented in chapter 1 (WG1) of this e-book [1] shows (i) the need for estimating the sound reduction index R* (for resonant transmission only) of lightweight building elements and the importance of the radiation efficiencies in this estimation and (ii) the need for an appropriate definition (and associated measuring method) of the junction vibration attenuation between connected lightweight elements. This paper proposes methods for measuring the radiation efficiency of lightweight elements as well as for measuring and characterizing the velocity level difference of junctions between lightweight elements. Examples of measurement results are given. The principles of these methods have already been presented in a paper [2], which content has been up-dated taking into account more recent studies.

3.1 - Radiation efficiencies

3.1.1 - Measuring method

In building acoustics, the radiation efficiency σ of a building element is defined from the following expression of the power radiated:

$$\Pi_{rad} = \rho c \sigma . S < v^2 > \qquad (1)$$

where ρc is the air impedance, S the surface area of the element and $<v^2>$ the space average velocity of the element.

This radiated power can be measured in a room of absorption area A from the space average sound pressure $<p^2>$ in the room:

$$\Pi_{rad} =< p^2 > .A/4\rho c \qquad (2)$$

Equations (1) and (2) are power based expressions assuming diffuse field in both structure and room. Expressed in dB in terms of sound level L_p (ref. 2 10^{-5} Pa) and velocity level L_v (ref. 5 10^{-8} m/s), (1) and (2) lead to:

$$10\log(\sigma) = L_p - 6 - L_v + 10\log(A/S) \qquad (3)$$

From equation (3), the following measurements method can then be proposed, knowing that low frequencies (below 100 Hz) are important, especially in lightweight buildings:

Sound pressure measurements: L_p and A can be measured according to ISO 140 Part 3, [3], which includes an annex for low-frequency measurements down to 50 Hz. Other methods adapted to low-frequency measurements such as the method developed for field

measurements in smaller rooms [4] or the laboratory method based on acoustical intensity measurements [5] would probably give more accurate results.

Vibration measurements: L_v can be measured using the same method as when measuring the velocity level difference of junctions between elements (see section 2 of this paper)

The radiation efficiency depends on the type of excitation used (airborne or mechanical excitation) leading, in the case of lightweight elements to two different spectra for the radiation efficiency (σ_a and σ_r respectively). An airborne excitation (as in ISO 140 Part 3) will be uniformly distributed over the element, thus generating a rather diffuse vibrational field. In the case of mechanical excitation, only several positions of the tapping machine (as is ISO 140 Part 16, [6]) or "rain on the roof" hammer impacts can generate a uniformly distributed excitation.

The radiation efficiency eventually depends on which side of the element the power radiated is measured (see example below)

3.1.2 - Examples of results

The radiation efficiency of a two board single leaf wall (gypsum board BA13 + OSB) on (120 x 45) wooden studs is shown in Figure 1 in the two cases of airborne and mechanical excitation, the radiated power being measured either on the stud side or on the board side.

The results show that a difference of 10 dB can be found in the low frequency range between airborne and mechanical excitation, showing the importance of the correction term in equation (2) in the proposal for acoustic prediction given in the e-book first chapter [1]. This difference decreases near critical frequency (3150 Hz for the lightweight element presented here). Only small differences in radiation efficiency can be seen between the radiation sides (plate or studs). In the case of heavy building elements (low critical frequency), higher values of radiation efficiency would be found at low frequencies and results practically independent of the excitation (airborne or mechanical) would be obtained over the whole frequency range.

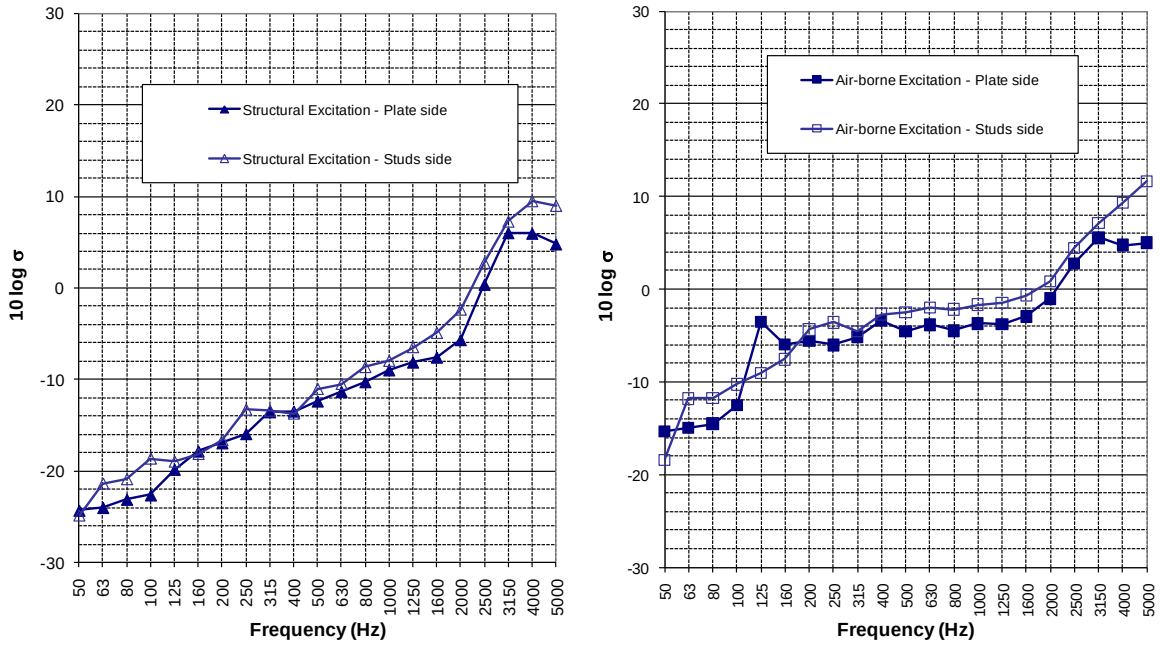

a) b)

Figure 1: Measured radiation efficiency of a single leaf wall in the cases of (a) mechanical excitation and (b) airborne excitation.

3.2 - Junction velocity level difference

3.2.1 - Measuring method

The standard EN 10848 series [6] specifies laboratory measurement methods for characterizing flanking transmission of airborne and impact noise between adjoining rooms. According to this standard, two approaches can be used:

(i) the flanking path considered can be characterized by a flanking level difference $D_{n,f}$ and a flanking impact sound level $L_{n,f}$, each transmission path being separated by shielding (see Figure 2); according to the standard, this approach can be applied to any type of structures, including lightweight elements; but shielding is cumbersome (also true for heavy elements), might affect the behaviour of the lightweight elements involved in the junction considered and might not be efficient enough at low frequencies around and below 100 Hz (also true for heavy elements). Note that $D_{n,f}$ measurements require an airborne excitation in the emission room. This approach has been used by laboratories such as NRC in Canada [7] and EMPA in Switzerland [8].

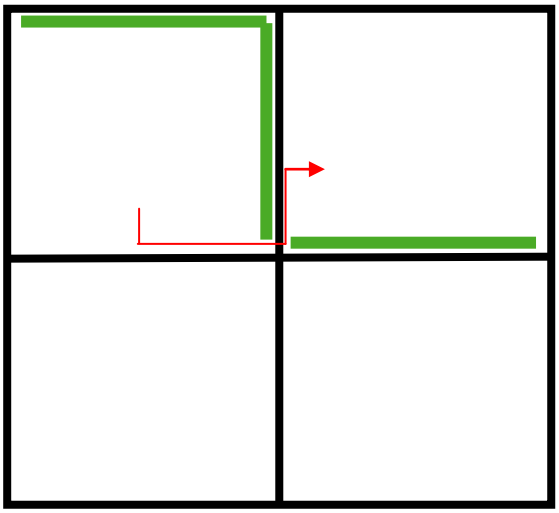

Figure 2: Example of shielding in the measurement of a particular flanking transmission path between two rooms

(ii) the flanking path considered can be characterized by a vibration level difference $D_{vs,ij}$ (the *s* subscript stands for structural excitation) from which an invariant (the vibration reduction index K_{ij}) of the junction is calculated. According to the standard, this K_{ij} approach and the related measurement methods are only valid with the assumption of a diffuse structural field which is not the case for lightweight and usually highly damped structures. In the standard, a condition of diffusivity is given in terms of vibration attenuation with distance, which should not exceed 6 dB across the element; the examples given in [2] show that this condition is rarely fulfilled in lightweight elements.

However, the notion of vibration level difference still makes sense with lightweight elements as explained in reference [9], which shows that first order SEA, on which the EN 10848 series is based, can still be applied to lightweight constructions, but only if the mechanical excitation is uniformly distributed over the emission plate (using several tapping machine positions for floors or "rain on the roof" hammer excitation for walls) and if the vibration fields are measured with a sufficient number of accelerometer positions (between 10 and 15, depending on the element size), and located over the whole element. Figure 3 shows a typical floor/wall X junction (top view), where the source positions are indicated as well as the vibration attenuation with distance in the receiving element (stronger with increasing frequencies). For a measured junction length l_{ij}, the structural power transmitted is proportional to the product $S_{m,j} <v^2>$, which must stay the same in the field prediction when estimating the sound pressure radiated (the *m* subscript stands for measurement area). An invariant for lightweight element junctions can then be defined as the following normalized direction average velocity level difference:

$$\overline{D_{v,ij,n}} = (D_{v,ij} + D_{v,ji})/2 + 10\log(l_{ij}/\sqrt{S_{m,i}.S_{m,j}}) \qquad (4)$$

from which the in situ direction average velocity level difference of a similar junction can be calculated as

$$\overline{D_{v,ij,situ}} = \overline{D_{v,ij,n}} - 10\log(l_{ij,situ} / \sqrt{S_{situ,i}.S_{situ,j}}) \quad (5)$$

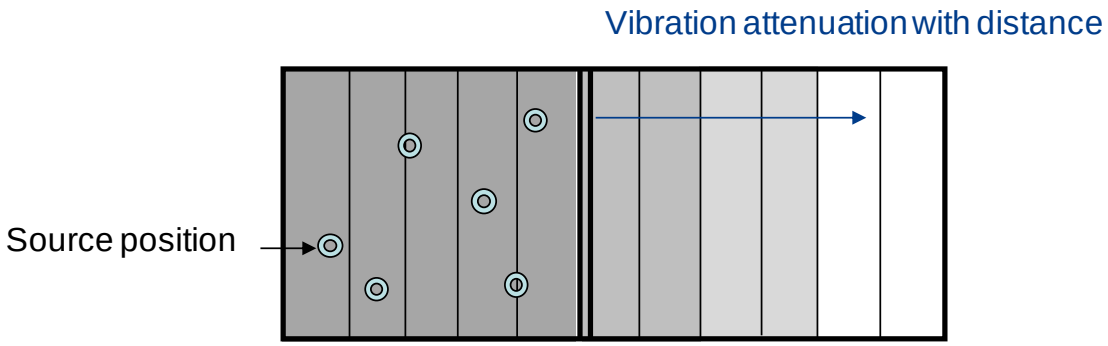

Figure 3: Top-view of a lightweight floor/wall junction with joists // junction

It should be noted that measuring the energy stored in a lightweight element ($S<v^2>$) generated by a known structural power injected might be a way of characterizing an apparent loss factor. Such method is proposed in a research study [10] on comparing structure borne noise from waste water installation in heavy and lightweight constructions.

3.2.2 - Examples of results

The normalized velocity level differences of a lightweight floor-wall X junction composed of a 25mm CTBH floor on wood joists (joist parallel to junction) and a single frame double wall (18 mm gypsum board on one side and 10 mm OSB on the other) are shown in Figure 4; the 3 paths (floor-floor, wall-wall and floor-wall) are given.

The results show that higher values of velocity level differences are obtained, compared to heavy junctions, and the slopes are stronger (stronger increase of velocity level difference with increasing frequencies).

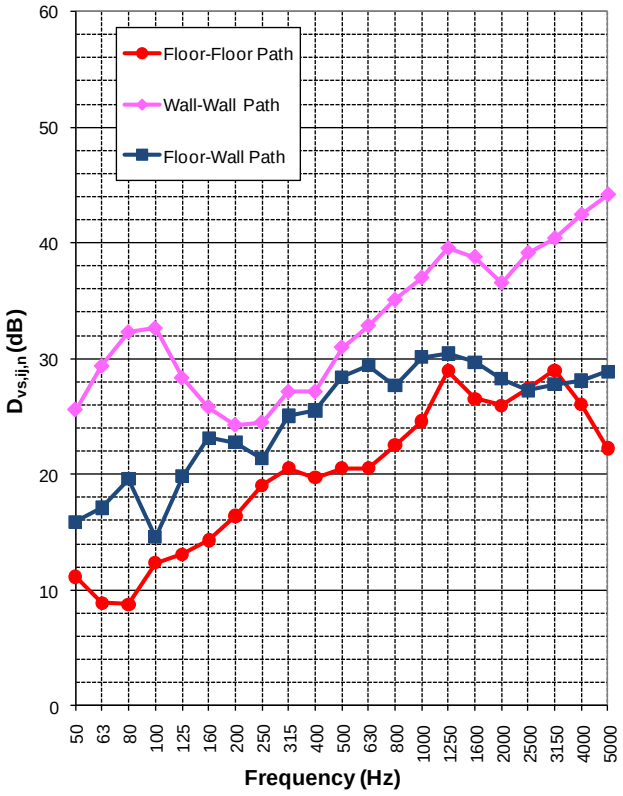

Figure 4: Measured normalized velocity level differences of a lightweight floor-wall X-junction.

3.3 - Conclusion

The above proposals for defining, measuring and characterizing the radiation efficiency of lightweight elements and the velocity level difference of junctions between lightweight elements can sure be further tested and improved, and will hopefully help the CEN/TC126 working groups prepare the corresponding (and missing) European standards.

3.4 - References

[1] "Final proposal for prediction of acoustic performances in lightweight buildings", COST Action FP0702, e-book Chapter 1 (WG1-Prediction methods for sound and vibration performances, including low frequencies), 2012.

[2] M. Villot, C. Guigou-Carter, "Measurement methods adapted to wood frame lightweight constructions", Building Acoustics, Volume 13, Number 3, 2006

[3] ISO 140, Acoustics – Measurement of sound insulating in buildings and of building elements – Part 3: Laboratory measurement of airborne sound insulation of building elements, 1995

[4] C. Hopkins, "New proposal for field measurements in the low-frequency range", COST Action FP0702, e-book Chapter 2 (WG2-Measurement methods for sound and vibration performances, including low frequencies), 2012.

[5] ISO 15186, Acoustics - Intensity measurement of sound insulating in buildings and of building elements – Part 3: Laboratory measurement at low frequencies, 2011

[6] ISO 10848 series (Parts 1 to 4), Acoustics, Laboratory measurement of the flanking transmission of airborne and impact noise between adjoining rooms

[7] S. Schoenwald, "Prediction of flanking sound transmission in lightweight building structures with SEA – Conclusions for a standardized prediction method", *Proc. Inter-noise 2009*, Ottawa, Canada

[8] C. Geyer, H.-M. Tröbs, R. Bütikofer, L. Krajči, "Measurements of flanking transmissions using a newly developed radiation efficiency measurement method in a flanking transmission suite", *Proc. Euro-noise 2012*, Prague, Czech Republic

[9] M. Villot and I. Bosmans, "Modeling and characterizing flanking transmissions in lightweight constructions", *Proc. Inter-noise 2002*, Dearborn, MI USA

[10] M. Villot and S. Bailhache, "Structure borne noise from waste water installation in heavy and lightweight constructions", *Proc. ICSV19 2012*, Vilnius, Lithuania

4 - MEASUREMENTS OF FLOOR DEFLECTIONS

Document written by Anders Homb
SINTEF Building & infrastructure, Norway

4.1 - Definition

In this document, the floor deflection is the measured deflection of the floor on the beams at the center (weakest point) of the span width with a point load of 1,0 kN.

4.2 - Measurement setup

4.2.1 - Principle

The beam floor construction has to be applied with a point load of 1,0 kN on the floor directly above a beam at the center of the span width. The deflection due to this load has to be measured in the same position, at the support and on one or more neighboring beams. The principle is shown in figure A-1. The positions of the beams have to be determined within an accuracy of approximately ± 5 mm. When the floor has a rather high transverse stiffness (perpendicular to the main beam direction), it is recommended to make measurements on at least 5 beams with a center distance of 0,6 m. It is necessary to establish a reference system for the deflection measurements to ensure that the values are independent of the load at the different measurement positions, see ch. 2.2.

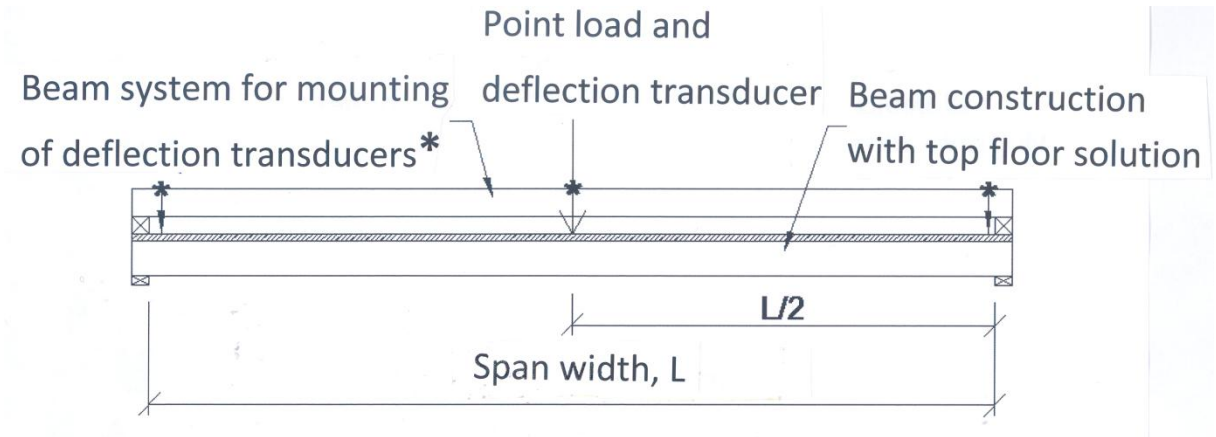

Figure A-1. Deflection measurements of beam floor construction

If possible, it is recommended to preload the floor construction in 2 to 6 minutes with a load comparable with load from normal use of the floor before the deflection measurements. An alternative is to put a number of dynamic loads into to floor, for instance heavy jumping on the floor.

4.3 - Reference system

The deflection transducers have to be mounted on a reference (beam) system. The stiffness of this system has to be adequate to avoid inaccuracy and movements of the transducers. It is necessary to establish the system in a way that avoids movements (from loading and unloading) at the support of the reference system. If the reference system is mounted above the floor, it will normally be safest to install the reference beam in the same direction as the floor beams with support as close as possible to the beam support. If the edges of the floor are sufficient stiff, the reference beam can be installed in the transverse direction of the floor beams.

4.4 - Point load

A person (additional mass included) can be used giving a total weight of 1 kN. An accuracy of 10 N of the load is acceptable. A support plate of 100 mm x 100 mm should be used between the floor (above the beam) and the point load. The load moves on and off the support plate minimum three times, with a recommended loading time of 20 sec.

If the measured deflection is below approximately 10 times the assumed measurement accuracy, we recommend to make measurements with increased point load, for instance + 500 N. Afterwards, the measurement results should be normalised to a point load of 1 kN.

4.5 - Measurement equipment

Electronic deflection transducers should be used with a resolution of 0,01 mm or better. The accuracy of the transducer (and registration system) should be calibrated regularly.

4.6 - Procedure

Values from the measurement system have to be registered before, at and after loading of the point, at least three times for each load position. If an unexpected change of the values occurs (at the same load point), the reason has to be clarified and the number of load cases has to be increased. It is necessary to chose minimum three load positions at the beam construction. If the deflection at the support increase 0,01 mm, it is recommended to improve the mounting of the reference system and redo the measurements.

4.7 - Results

The deflection of the beam construction is the average of the number of deflection results from each point load of 1,0 kN. Significant diverging values should be excluded from the averaging process.

4.8 - References

[1] Homb, A. (2008). Vibration properties of massive wood elements. *Project Report 24:2008, SINTEF Building & Infrastructure.* Oslo 2008 (in Norwegian).

[2] Hu, L.J. (2007). Design Guide for Wood-Framed Floor Systems. *Report no. 32 to Canadian Forest Service.* Final Report 2006/2007. Forintek Canada Corp., 2007.

[3] Homb, A. (2006). Low frequency sound and vibrations from impacts on timber floor constructions. *Doctoral theses at NTNU, 2006:132.* IME Faculty, Dep. of Electronics and Telecommunications, Trondheim, Norway.

[4] Toratti, T. and Talja, A. (2006). Classification of Human Induced Floor Vibrations. *Building Acoustics, 2006.* **13**(3): p. 211-221.

[5] EuroCode-5 (2005). Design of timber structures - Part 1: General rules and rules for building. Brussel s 2005.

[6] Homb, A. (2000). Floor vibrations and low frequency sound pressure levels using a rubber ball impact method. *Proceedings Inter.noise 2000*, Nice 27-30. august 2000, France.

[7] Dolan, J.D., Murray, T.M., Johnson, J.R., Runte, D. & Shue, B.C. (1999). Preventing Annoying Wood Floor Vibrations. *Journal of Structural Engineering,* Vol. 125, No. 1, 1999, pp. 19-24.

[8] Ohlsson, S.(1988). Springiness and human induced Floor vibrations. A design guide. *Report D12:1988, Swedish Council for Building Research*, Stockholm, 1988.

[9] Blevins, R.D.(1979). Formulas for natural frequency and mode shape. *Van Nostrand Reinhold, New York*, 1979.

[10] Leissa, A.(1969). Vibration of plates. *NASA SO-160,* Washington DC, 1969.

5 - HOW TO MEASURE FLOOR LOW FREQUENCY VIBRATION

Document written by Nathalie Labonnote
Norwegian University of Science and Technology, Trondheim, Norway

5.1 - Experimental modal analysis

Experimental Modal Analysis (EMA) is the field of measuring and analyzing the dynamic response of a structure when excited by a stimulus. The stimulus can consist of either a continuous periodic excitation provided by a shaker, or of an impact load, generally provided by a modal hammer. The vibration response of the structure is recorded by means of vibration sensors, usually accelerometers, which have to be located strategically on the structure in order to reveal its vibration modes. Specialized data acquisition hardware providing proper signal conditioning is needed to properly acquire these vibration signals. The frequency response function (FRF) compares the stimulus and response to calculate the transfer function of the structure. The result of the FRF is the structure's magnitude and phase response over a defined frequency range. It shows critical frequencies of the structure that are more sensitive to excitation. Those critical frequencies are the modes of the structure under test. Modal parameter extraction algorithms are used to identify the modal parameters from the FRF data.

Modal analysis issues have been extensively reviewed by Ewins [1] and Maia [2] , and excellent vulgarization has been provided by Schwarz and Richardson [3]. The relative advantages and drawbacks of shaker excitation versus modal hammer excitation have been reviewed by Reynolds and Pavic [4]. What follows is a general summary of information collected from the previously cited reviews.

5.1.1 - Modal hammer testing

Hammer testing is the most commonly used technique, since it is quick, easy and relatively cheap. The convenience of this technique is attractive because it requires very little hardware and provides shorter measurement times. Indeed, the only equipment needed is a modal hammer, shown in *Figure 5.1*, and an accelerometer, shown in *Figure 5.3*. In addition, the measurement method is fully portable, and therefore highly suitable for field work. When the modal hammer tip hits the structure, a wide frequency range is quickly excited. Hammer testing is decried mainly because of the lack of repeatability. The input force may indeed vary because of different operators, or difficult location. In addition, high crest factor due to impact may drive the structure into non-linear behavior. And since large structures require high peak force to be set into motion, there is always a risk of local damage. For instance, hammer testing is not recommended for composite testing.

Since the force is an impulse, the amplitude level of the energy applied to the structure is a function of the mass and the velocity of the hammer. Since it is difficult to control the

velocity of the hammer, the force level is usually controlled by varying the mass. Impact hammer are available in weights varying from some grams to several kilograms, in order to allow the testing of different structures.

Figure 5.1: The modal hammer used for all experimental studies

The frequency bandwidth is inversely proportional to the pulse duration. In addition, the magnitude and pulse duration depends on:

- the weight of the hammer
- the hammer tip: steel, plastic or rubber
- the dynamic characteristics of the surface
- the velocity at impact

It is not feasible to change the stiffness of the tested structure; therefore the frequency content is controlled by varying the stiffness of the hammer tip. The harder the tip, the shorter the pulse duration and thus the higher the frequency content, as illustrated in *Figure 5.2*.

In general, small low-mass objects have higher response frequencies and thus require higher frequencies of excitation at lower force levels. Heavier structures with lower fundamental frequencies require lower frequency excitation at higher input force levels.

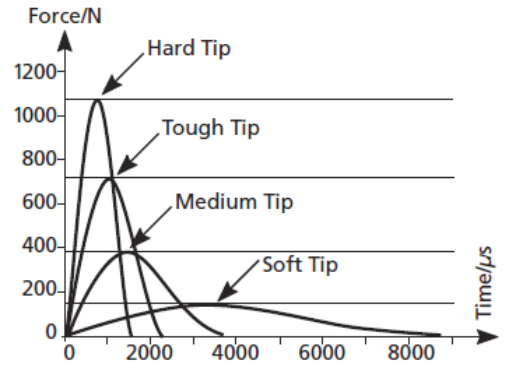

Figure 5.2: Impulse shapes of the modal hammer as a function of used impact tip [5]

5.1.2 - Shaker testing

Shaker testing is often used in more complex structures, and comprised many different excitation techniques. The structure is set into motion by "shaking" it, which is more repeatable than hammer testing, but requires a skilled operator. In addition, particular attention needs to be given to the attachment of force transducers and shaker [6]. In

order to protect the shaker, which is expensive equipment, the force transducer is attached to the structure, and linked to the shaker via a connection rod, also called stinger. The stinger exhibits a high axial stiffness and a low bending stiffness, so that the excitation force acts only at the desired point and in the desired direction. In addition, the structure is free to vibrate with no moment excitation and no rotational inertia loading.

The chosen method for supporting the shaker may affect the force imparted to the structure. The main body of the shaker must be isolated from the structure to prevent any reaction forces from being transmitted through the base of the shaker back to the structure. This can be accomplished by mounting the shaker on a solid floor and suspending the structure from above. The shaker could also be supported on a mechanically isolated foundation. Another method is to suspend the shaker, in which case an inertial mass usually needs to be attached to the shaker body in order to generate a measurable force, particularly at lower frequencies. The location of the shaker is of great importance in order to minimize the amplitude of undesirable modes [7].

Different excitations may be implemented through a shaker. The sine excitation is best for studying non-linearities under the form of harmonic distortion. For broadband excitation, the sine wave is slowly swept through the frequency range of interest, under quasi-stationary condition. This process is therefore very slow. The random excitation consists of a random variation of amplitude and phase, and has the advantage of averaging. In other words, this gives optimum linear estimate in case of non-linearities. The random signal is characterized by a power spectral density and an amplitude probability density, which means it can be limited according to the frequency range of interest. Other types of excitation signals, such as burst random, pseudo-random, multisine, periodic random, or periodic pulse are studied in detail by Schwarz and Richardson [3].

5.1.3 - Operational modal analysis

Operational modal analysis uses the natural and ambient excitation of the structure. It is still a cutting edge technique, sometimes the only solution for very large structures e.g. long bridges, for which a huge amount of energy would have to be implemented by classical techniques of shaker or modal hammer. Since it is an in-situ measure, there is no need for special boundary conditions, and other tests may be performed in the same time. It is nevertheless a computation intensive measurement method, and it has to be ensured that the natural excitation covers the frequency range of interest. More importantly, there is no control of the excitation, and uncertainties must therefore be carefully taken into account.

5.1.4 - Vibration sensors

Vibration sensors may differ in number, depending on the experimental protocol. Very often the vibration sensor is an accelerometer, but sometimes a displacement transducer

may be used. Accelerometers may be fixed to the structure via a threaded stud as shown in *Figure 5.3*, but may also use some cement, wax, or even magnetostatic forces.

5.1.5 - Experimental protocols

Various experimental protocols may be used, depending on the number of recorded inputs and outputs. The Single Input Single Output (SISO) measurement system is usually related to hammer testing, and consist of recording the vibration response at a single location, with the structure being excited at a single location. An extension of this method is used for the roving hammer method, which consists of several SISO measurements on a finite and predefined number of measurement points. A special case of SISO measurement system is the driving point method [8], which consists of recording the vibration response at the same single location where the structure is excited. The driving-point measurement on large structures can normally be performed, without introducing any significant errors, by applying the excitation very close to the transducer [9]. On small structures it is often possible to attach the force and driving-point transducers on opposite sides of the structure at the excitation point.

The Single Input Multiple Output (SIMO) measurement system consists in recording the vibration response at several locations, simultaneously, with the structure being excited at a single location. This is also compatible with the roving hammer method, which is that case would consist in several SIMO measurements on a finite and predefined number of measurement points. SIMO is also popular for shaker testing. It is common that in that case, all predefined measurement points are equipped with a vibration sensor, so as to optimize data consistency.

The Multiple Input Multiple Output (MIMO) measurement system consists in recording the vibration response at several locations, simultaneously, with the structure being excited at a several locations, simultaneously. Multiple inputs are required for large and complex structures in order to get the excitation energy sufficiently distributed, and in order to avoid non-linear behavior.

Figure 5.3: Accelerometer mounted using a double sided threaded stud

Lastly, the Multiple Input Single Output (MISO) measurement system consists in recording the vibration response at a single location, with the structure being simultaneously excited at several locations.

5.1.6 - Frequency Response Function

The full frequency response matrix **H** may be written as:

$$\begin{Bmatrix} X_1 \\ X_2 \\ \vdots \\ X_n \end{Bmatrix} = \begin{bmatrix} H_{11} & H_{12} & \dots & H_{1n} \\ H_{21} & H_{22} & \dots & H_{2n} \\ \vdots & \vdots & \vdots & \vdots \\ H_{n1} & H_{n2} & \dots & H_{nn} \end{bmatrix} \begin{Bmatrix} F_1 \\ F_2 \\ \vdots \\ F_n \end{Bmatrix} \qquad (1)$$

H_{ij} terms may be defined as:

$$H_{ij}(\omega) = \frac{X_i(\omega)}{F_j(\omega)} = \frac{\text{Response "}i\text{"}}{\text{Excitation "j"}} \qquad (2)$$

where $X_i(\omega)$ = Fourier transform of the response $x_i(t)$, and $F_j(\omega)$ = Fourier transform of the excitation $f_j(t)$. An example of experimental frequency response function is shown in *Figure 5.4*.

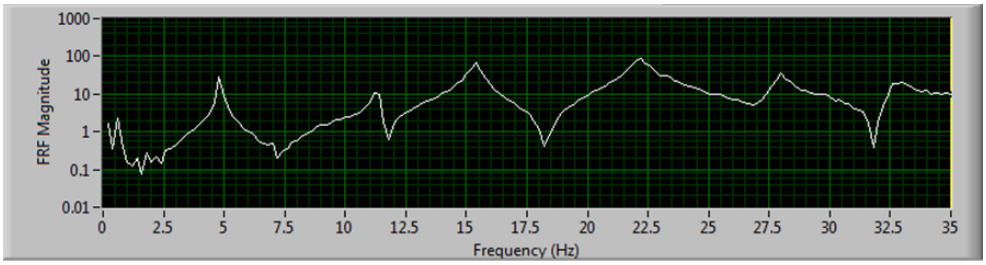

Figure 5.4: Experimental frequency response function

The knowledge of a unique row (from hammer testing), or of a unique column (from shaker testing), is usually enough to determine all the vibration modes of the system. For instance, the roving hammer method gives the knowledge of a unique row (SISO), or of several rows (SIMO), whereas the shaker testing method gives the knowledge of a unique column (SIMO). The driving point method determines one diagonal element of the frequency response matrix **H**.

The knowledge of a unique row or column from the frequency response matrix is not sufficient for determining all the vibration modes of the system when there are several modes for the same frequency, e.g. for symmetrical structures. In case of hammer testing, more locations for recording the vibration response are therefore required to increase the number of known rows. In case of shaker testing, the shaker has to be moved to different excitation locations in order to increase the number of know columns.

Experimental modal analysis is a linear theory. The frequency response function is therefore linear, i.e.:

$$\begin{cases}\{\mathbf{X}\}=\mathbf{H}\{\mathbf{F}\}\\ \{\mathbf{X}'\}=\mathbf{H}\{\mathbf{F}'\}\end{cases}\Rightarrow\begin{cases}\{\mathbf{X}+\mathbf{X}'\}=\mathbf{H}\{\mathbf{F}+\mathbf{F}'\}\\ a\{\mathbf{X}\}=\mathbf{H}\{a\mathbf{F}\}\end{cases} \quad (3)$$

The validity of the frequency response function is assessed by the coherence function γ^2, defined as:

$$\gamma^2(\omega)=\frac{\left|G_{XF}(\omega)\right|^2}{G_{FF}(f)G_{XX}(f)} \quad (4)$$

where G_{XF} = cross-spectral density, G_{FF} = load signal spectral density, G_{XX} = response signal spectral density. The coherence function is analogous to the squared correlation coefficient used in statistics, and measures the degree of linear relationship between the input and output signals at each fundamental frequency. A value close to one shows therefore good coherence. Coherence values lower than 0.75 are commonly considered poor, and may be due to noise in the measured output or input signal. Poor coherence may also be due to other input which would not be correlated with the measured input signal. By averaging several time records together, statistical reliability can be increased and random noise associated with nonlinearities can be reduced.

5.1.7 - Modal parameters extraction

Curve fitting is the process of estimating the modal parameters from the frequency response function evaluations. This is done by minimizing the squared difference between the assumed analytical function and the measured frequency response function. The modal parameters for all modes within the frequency range of interest constitute a complete dynamic description of the structure. Any free or forced dynamic response of a structure may be reduced to a discrete set of modes. The modal parameters are:

- Modal frequency
- Modal damping
- Mode shape

Suitable analytical expressions to curve fit the frequency response function with may be written as:

$$H_{i,k}=\sum_{r=1}^{n}\frac{(\psi_i\psi_k)_r}{\left[\omega_r^2-\omega^2+2j\xi_r\omega_r\omega\right]}$$

$$\text{with}\begin{cases}(\psi_i\psi_k)_r=\text{residues}\\ \omega_r=\text{undamped natural frequency}\\ \xi_r=\text{equivalent viscous modal damping ratio}\end{cases} \quad (5)$$

where *r* = mode number, and *n* = total number of modes. The undamped natural frequency and the viscous modal damping ratio are directly extracted from Eq. (5). The mode shapes vectors $\boldsymbol{\Psi}_r$ are extracted as:

$$\boldsymbol{\Psi}_r = \left[\left\{ \psi_1^2 \right\}_r \quad \left\{ \psi_1 \psi_2 \right\}_r \quad \cdots \quad \left\{ \psi_1 \psi_{13} \right\}_r \right] \qquad (6)$$

Single-degree-of-freedom (SDOF) methods estimate modal parameters one mode at a time, whereas multiple-degree-of-freedom (MDOF) methods can simultaneously estimate modal parameters for several modes, as shown in *Figure 5.5* a) and b), respectively. Local methods are applied to one frequency response function at a time, whereas global methods are applied to an entire set of frequency response functions. In general, local SDOF methods are the most convenient to use.

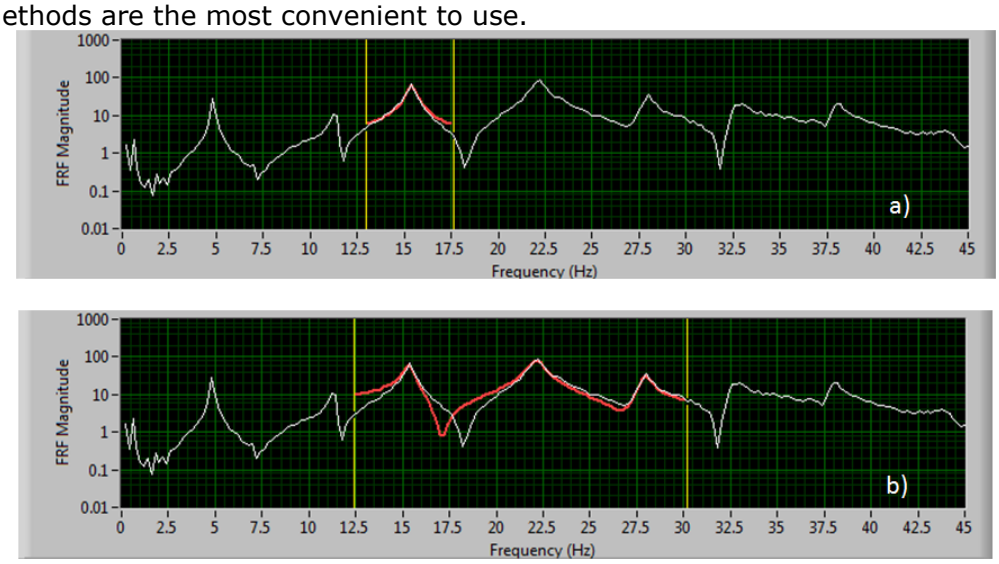

Figure 5.5: Curve fitting of frequency response function a) SDOF method b) MDOF method

SDOF methods are appropriate for lightly coupled modes, whereas multiple-degree-of-freedom MDOF methods are appropriate on heavily coupled modes. More detailed specific methods are described by Ewins [1].

Algorithms for fitting the analytical expressions are numerous, and are not further detailed here. An exhaustive review can be found from Srikantha Phani and Woodhouse's work [10], where they collected and compared different identification methods. Two years later, they applied the collected methods to experimental data [11]. They quantified and compared the performance of each method. For both studies, they considered three different groups:

- matrix methods, which are based directly on the FRF matrix, and give as outputs the mass, stiffness and damping matrices.
- modal methods, which use complex mode shapes and fundamental frequencies identified from modal testing, as defined in Section 5.1 - . In some cases, the

knowledge of the mass and stiffness matrices is brought by the finite element method

- enhanced methods, defined as possible improvements of matrix methods.

5.2 - Performed experimental studies

5.2.1 - Chosen experimental protocol

The modal hammer "heavy duty type 8208" from Brüel & Kjær, shown in Figure 5.1 was used to set the beam into motion. A soft tip was employed in order to excite lower frequencies. Transient vibrations due to modal hammer impact were recorded by one ceramic/quartz impedance head Kistler accelerometer type 8770A50 screwed into the timber structure, as shown in Figure 5.3. The load and acceleration time series were then digitalized and processed by a dynamic analyzer of signals. An experimental modal analysis software was provided by National Instruments [12] to record and process the data, using the graphical development environment LabVIEW. The sampling frequency was fixed to 1000 Hz (beams and floors) or 2048 Hz (panels), and 5 s data were recorded for each impact. A linear average of the estimated Frequency Response Function over 3 impacts (beams) or 2 impacts (panels and floors) was performed for each evaluation.

The present method is considered as non-destructive since the hammer impact is soft enough not to inflict any damage the structure or modify its properties. This also allows for an unlimited number of repeated measurements to be performed on each specimen.

Experimental Modal Analysis was used for determining the fundamental frequencies, the damping ratios and the mode shapes of the timber beams, via a software [12] provided by National Instruments as well. The parameter identification method is based on the Frequency-Domain Direct Parameter Identification (FDPI) fitting method, which is a frequency domain multiple degree of freedom modal analysis method suitable for narrow frequency band and well separated modes.

5.2.2 - Timber beams

A total of 22 beams were tested [13]: 11 solid wood beams and 11 glulam beams. Each beam was simply supported with a symmetric overhanging. Supports used were constructed of either rigid steel tripods or sections of thick steel cylinders. Teflon sheets were added in between the timber beam and the steel supports in order to minimize friction and other sources of structural damping. The impact and the data recording took place at the same location, 2.5 m from one end of beam, following the driving point method. The experimental setup is displayed in *Figure 5.6*.

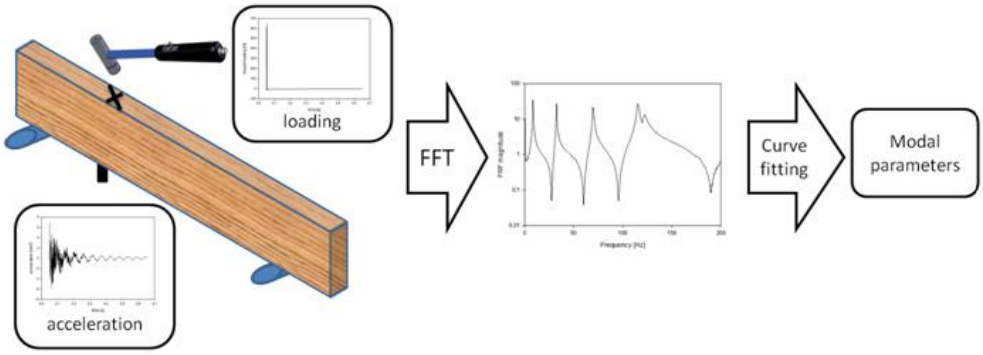

Figure 5.6: Driving point experimental setup for timber beams

Mode shapes of one glulam beam were evaluated following the roving hammer method. 13 measurement points were impacted along the beam, which corresponds to 50 cm spacing between consecutive points. The obtained three first mode shapes of a glulam beam, flatwise oriented, with a 5 m span are presented in *Figure 5.7*.

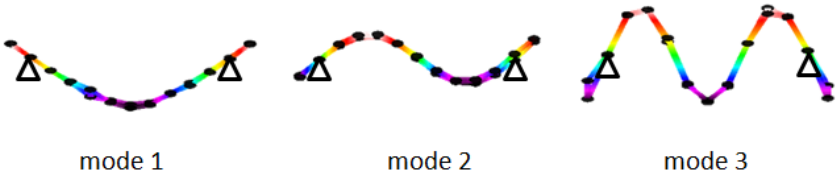

Figure 5.7: Experimental mode shapes of a glulam beam, flatwise oriented, with a 5 m span

5.2.3 - Timber panels

A total of 18 sheathing panels were tested [14]. Sheathing panels were either particleboard panels, Oriented Strand Board panels (OSB), or structural laminated veneer lumber panels (LVL). Steel cylinders whose outer diameter was 133 mm and whose thickness was 4 mm were used as supports, as shown in *Figure 5.8* a).

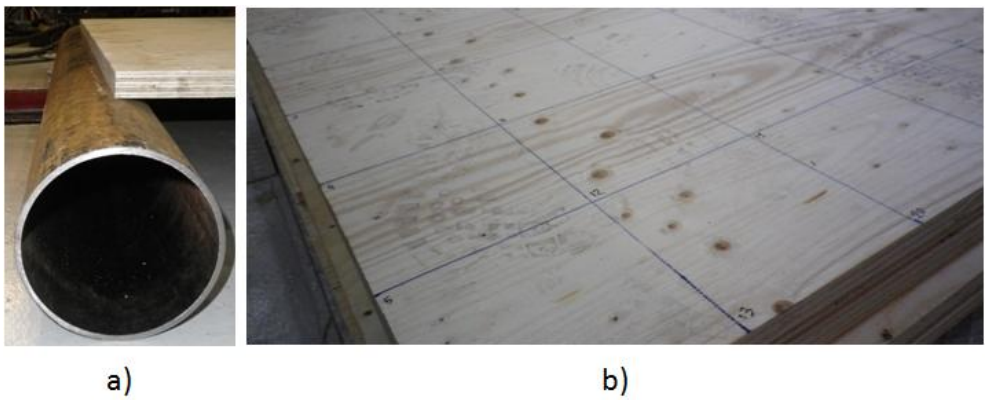

Figure 5.8: Experimental setup for timber panel testing a) supports b) discretization of the panel

Two different methods for evaluating dynamic properties of the sheathing panels were successively used. They are both illustrated in *Figure 5.9*. The unique location of both the accelerometer and the impact was designed so as to maximize the number of observed modes of vibration.

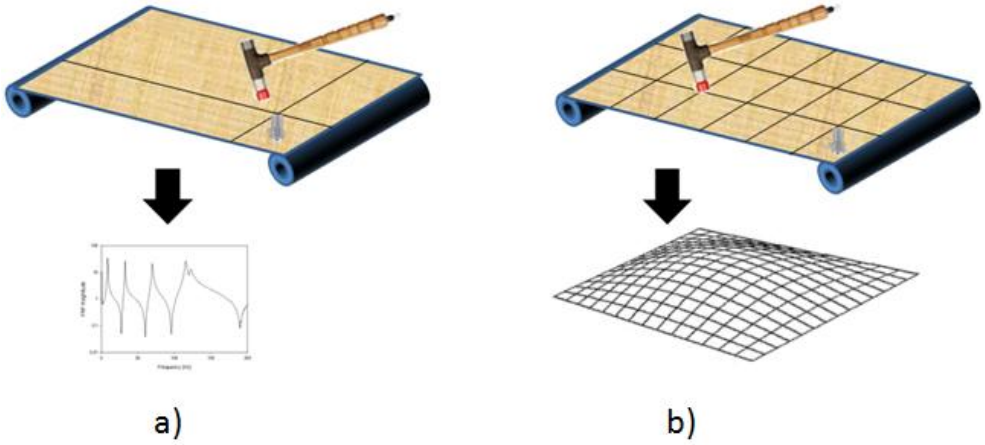

Figure 5.9: Timber panels experimentally evaluated by different methods: a) Driving point method and b) Roving hammer method

The mode shapes corresponding to each type of panel (given thickness and given material) were evaluated by means of the roving hammer method shown in *Figure 5.8* b), while the accelerometer remained at one unique location. The grid consisted of 84 to 91 measurement points, depending on the type of panel. This is equivalent to 20 cm to 25 cm spacing between each consecutive point. A total of 1484 measurements were performed. The obtained six first mode shapes for a 22 mm thick OSB panel, simply supported on short sides are presented in *Figure 5.10*.

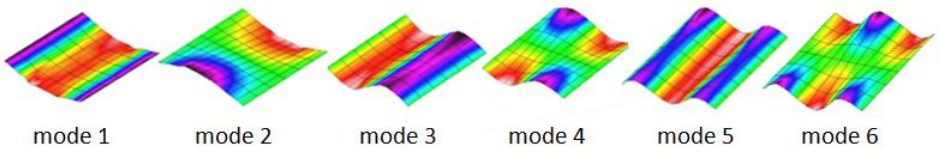

Figure 5.10: Experimental mode shapes for an OSB panels, simply supported on its two short sides

5.2.4 - Timber floors

Two timber floors were tested [15]: one whose connectors were all screws, one whose connectors were all nails. Both timber floors were simply supported on four corners, by means of 20 cm long steel cylinders located along the edge joists, as shown in *Figure 5.11*. A total of 784 measurements were performed.

The driving point method was first used to obtain modal damping and fundamental frequencies. The roving hammer method was then used to obtain the mode shapes. The grid consisted of 195 measurements points, which corresponds to a 20 cm spaced grid.

The first five modes for the timber floor assembled with screws, with the accelerometer located on a beam are shown in *Figure 5.12*.

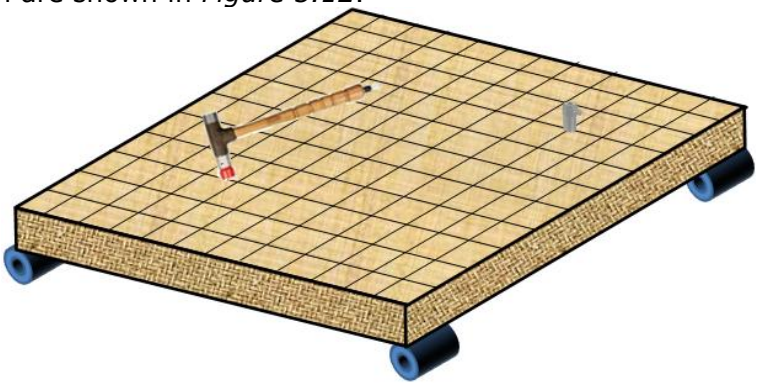

Figure 5.11: Experimental measurements on floors

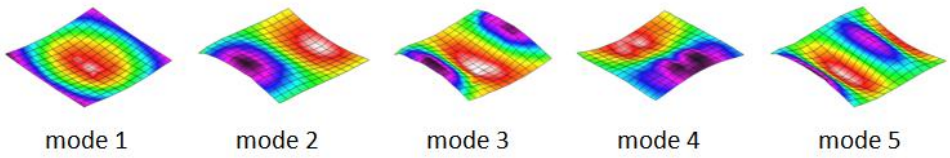

Figure 5.12: Experimental mode shapes of a floor simply supported at its corner

5.3 - Other methods for Experimental measurements of damping

There are different methods for estimating damping, using either time domain or frequency domain analysis. Accuracy of the estimation may vary depending on the prediction method, and is particularly influenced by the "noisiness" of the data.

5.3.1 - Logarithmic decrement

This is the simplest and most frequently used method for finding the equivalent viscous damping ratio through experimental measurements. When the system has been set into free vibration by any means, damping estimates can be made from the rate of decay of the transient response, as described in Figure 5.13. The logarithmic decrement δ is defined with respect to p consecutive cycles of vibration:

$$\delta = \frac{1}{p} \ln \frac{x_{n+p}}{x_n} \qquad (7)$$

The logarithmic decrement δ is dimensionless, e.g. a value of 0.1 means that the amplitude decreases of 10% in any consecutive cycle. A major advantage of the logarithmic decrement method is that equipment and instrumentation requirements are minimal; the vibrations can be initiated by any convenient method and only the relative

displacement amplitudes need to be measured [16]. The damping ratio ξ is then evaluated from:

$$\xi = \frac{\delta}{2\pi} \qquad (8)$$

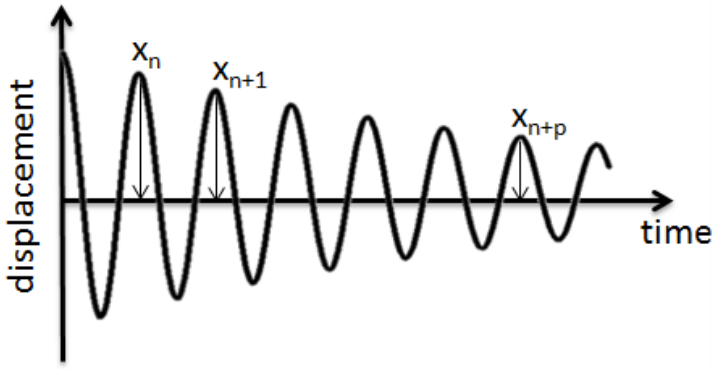

Figure 5.13: Transient response of an underdamped single-degree-of-freedom system and log decrement calculation

The simplicity of the method is its main advantage, and explains its broad use in damping investigations [17]. For instance, Obataya, Ono and Norimoto [18] used it for measuring damping in wood, Maslov and Kinra [19] for measuring the damping capacity of carbon foams, Gounaris et al. [20] for measuring the loss factor of a cantilever steel beam. If the damping is truly of viscous form, any set of consecutive cycles will yield the same damping ratio. However the damping ratio often is found to be amplitude dependent. This is of direct influence on the logarithmic decrement, since consecutive cycles in the earlier portion of high amplitude free vibration response will yield a different –often higher – logarithmic decrement than consecutive cycles in a later stage of much lower response. Caution must therefore be exercised [16]. Moreover, Cai et al. [21] reported that the consistency and repeatability of this method when applied to wood and wood-based materials were found lacking.

5.3.2 - Envelope fitting

Another widely used approach to determine damping from a free vibration curve is to fit an exponential curve passing though the peaks amplitudes, as presented in *Figure 5.14*. The decay profile is described by:

$$X(t) = Ae^{-\xi\omega_n t} \qquad (9)$$

where A = constant and ω_n = fundamental frequency. The envelope fitting approach yields a higher degree of accuracy compared to the logarithmic decrement method, since it takes into account all selected consecutive cycles, instead of only the first and the last of a series. The more peaks are used in the calculation, the better the evaluation of damping.

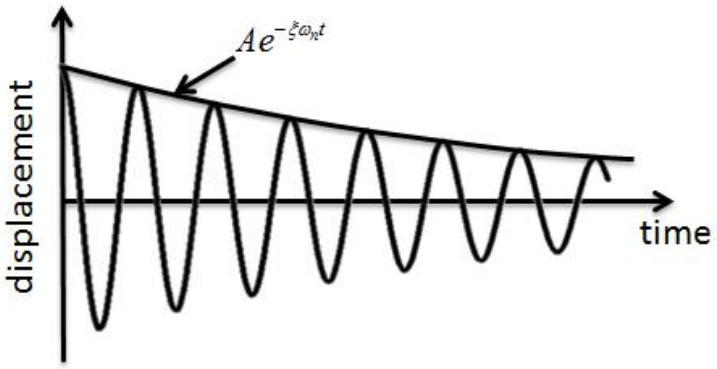

Figure 5.14: Envelope fitting of the transient response of an underdamped single-degree-of-freedom system

Though more accurate, the envelope fitting method yields a drawback similar to the logarithmic decrement method. If the damping is not of viscous form, the fitting of the envelope along the whole transient response is likely to be of limited quality. Besides, all points from the transient response contain damping information, but both methods use only a very small percentage of this available information, i.e. peak data only. Both methods are therefore limited in terms of efficiency. Another issue related to both methods is that they are both strongly dependant on the sampling rate used to collect data. The lower the sampling rate is, the worse the approximation of actual amplitudes is.

5.3.3 - Phase plot diagram

Cai et al [21] presented a different way to use the free vibration of a single-degree-of-freedom system. They used the $x - \dot{x}/\omega_n$ plane to plot the transient response, and obtained a spiral curve asymptotically approaching the origin. The radius *R* of the spiral curve in Figure 5.15 a), when plotted in the time domain, is the same as the decay profile curve of the free vibration. If the damping ratio ξ is less than 2%, the following relationship between the radius *R* and the damping ratio ξ can be written with an error not exceeding 1%:

$$R = \sqrt{x^2 + \frac{\dot{x}^2}{\omega_n{}^2}} = Ae^{-\xi\omega_n t} \qquad (10)$$

Taking the natural logarithm of Eq. (10) yields:

$$\ln R = \ln A - \xi\omega_n t \qquad (11)$$

A simple linear regression can therefore be used to find the slope, which in turn determines the damping ratio ξ. Since all sample points in the time domain are used, this procedure makes the maximum use of the available information and provides more accurate damping evaluations. When using this method, the damping ratio does not

depend on the initial amplitude and the phase, which are only contained in the intercept. Furthermore, the damping ratio does not depend on the time interval in which sample points are chosen for the linear regression because of the linearity.

Velocity is rarely directly measured during experiments, but can however be obtained either by numerical integration of acceleration (preferred) or numerical differentiation of displacement. Cai's method's accuracy is therefore dependent on the sampling rate, due to numerical manipulations on the signal.

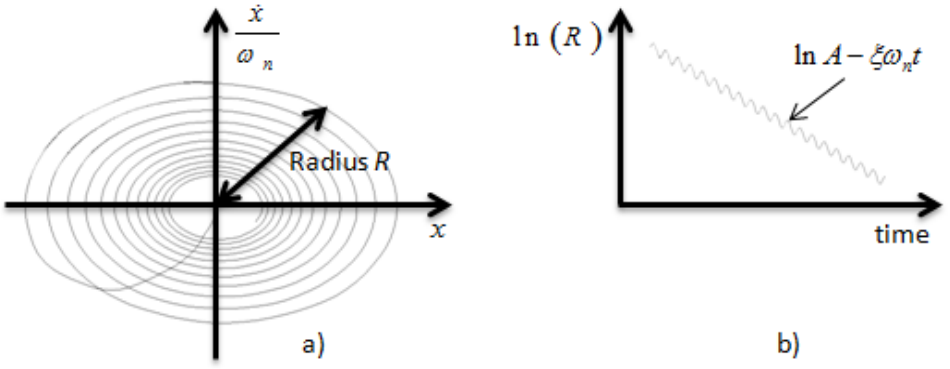

Figure 5.15: Cai's procedure: a) transient response of a single-degree-of-freedom in the phase plane b) linear regression

5.3.4 - Half-power bandwidth

The steady-state response of a vibrating system can also be used to evaluate damping. In such cases, the transfer function is preferred to any other representation of the signals. The level of damping can be subjectively determined by noting the sharpness of the peak: the more rounded the shape, the more damping [22]. The half-power bandwidth method achieves a quantitative evaluation of the hysteretic damping:

$$\eta = \frac{\Delta\omega}{\omega_0} \qquad (12)$$

where $\Delta\omega$ is determined from the half-power points ω_1 and ω_2 and from the resonant peak value ω_0, as illustrated in *Figure 5.16*. On a decibel scale, this corresponds to -3dB down from the peak value. The assumption of small damping [23] yields:

$$\eta = 2.\frac{\omega_1 - \omega_2}{\omega_1 + \omega_2} \qquad (13)$$

The half-power bandwidth method was used in many studies [18, 20, 24-27]. The hysteretic damping η provided by the half-power bandwidth method is extremely sensitive to the accuracy of peak location, which is itself highly dependent on the sampling rate. The half-power points ω_1 and ω_2 are dependent on both the accuracy of the peak location and the resolution of the transfer response, and therefore depend on the sampling rate as well.

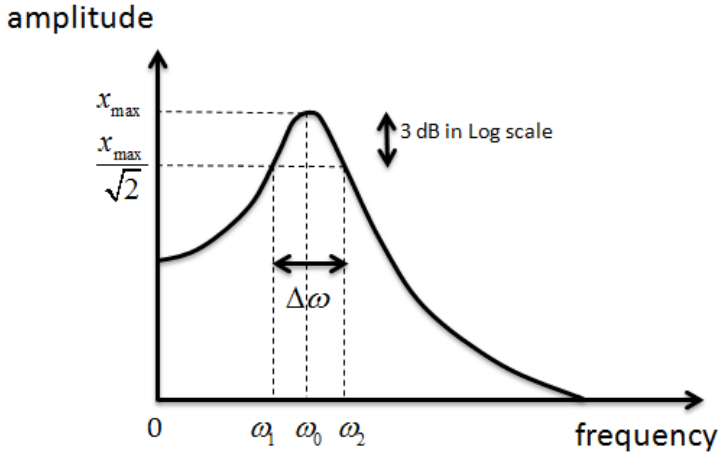

Figure 5.16: Half-power bandwidth method applied to the compliance transfer function of a single-degree-of-freedom system

5.3.5 - Resonant Amplification

The resonant amplification method is also based on the steady-state response of a vibrating system and its transfer function. The amplification factor Q is defined as the ratio of the response amplitude at resonance, ω_0, to the static response at $\omega = 0$, so that:

$$Q = \frac{x(\omega = 0)}{x(\omega = \omega_0)} = \frac{x_s}{x_{max}} \qquad (14)$$

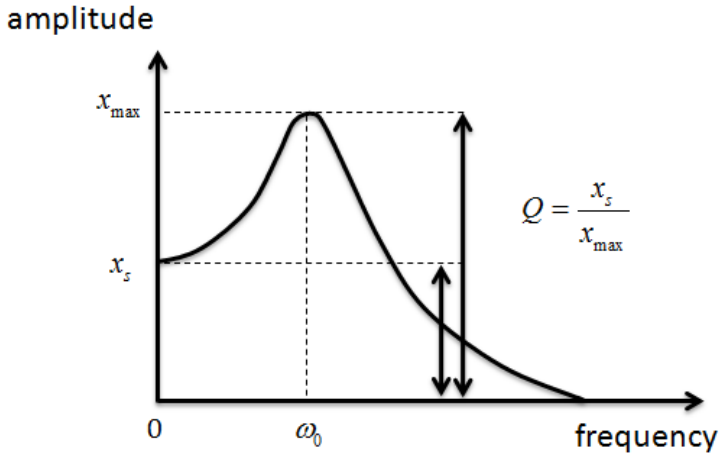

Figure 5.17: Resonant amplification method applied to the compliance transfer function of a single-degree-of-freedom system

This method of determining the damping ratio requires only simple instrumentation to measure the dynamic response amplitudes at discrete values of frequency and fairly simple dynamic loading equipment. Similarly to the half-power bandwidth method, it requires good resolution of the transfer function in the neighborhood of the peak. In addition, obtaining the static displacement may present a problem because the typical harmonic loading system cannot produce a loading at zero frequency [16].

5.3.6 - Resonant energy loss per cycle

Another evaluation of damping can be achieved by calculating the energy loss per cycle of oscillation under steady-state harmonic loading. This procedure involves establishing resonance by adjusting the forcing frequency until the displacement response is 90 ° out-of-phase with the applied loading. At resonance, the damping force f_D is exactly balanced by the excitation F [16]. The hysteresis loop is then defined by plotting the applied loading F versus the displacement x for one cycle of motion. If the system possesses linear viscous damping, as in *Figure 5.18* a), the hysteresis loop is an ellipse and the viscous damping ξ may be directly computed. Indeed:

$$F_{\max} = F_0 = f_{D,\max} = c\dot{x}_{\max} = 2\xi m\omega^2 X_0 \qquad (15)$$

Finally:

$$\xi = \frac{F_0}{2m\omega^2 X_0} \qquad (16)$$

If damping is of a non-linear viscous form, as in Figure 5.18 b), the hysteresis loop is not elliptical, because the response X is a distorted harmonic even though the applied loading F remains a pure harmonic. The area captured within the hysteresis loop, ΔE, is equal to the dissipated energy per cycle of harmonic motion by the system, and may be calculated as:

$$\Delta E = \pi F_0 X_0 \qquad (17)$$

The equivalent viscous damping ratio ξ_{eq} is then determined by:

$$\pi f_0 X_0 = \Delta E = \Delta E_{eq} = c_{eq}\pi\omega X_0^{\,2} = 2\xi_{eq} m\omega^2 X_0^{\,2} \qquad (18)$$

Finally:

$$\xi_{eq} = \frac{F_0}{2m\omega^2 X_0} \qquad (19)$$

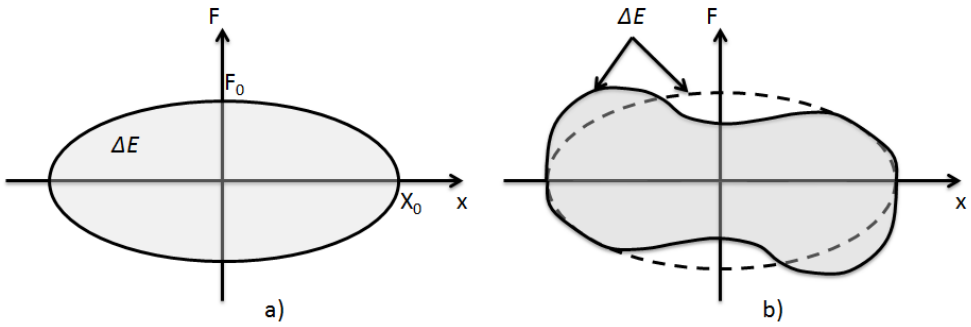

Figure 5.18: Hysteresis loops a) for a system of viscous damping form b) for an actual system

Implementing the resonant energy loss per cycle method requires to identify resonance, and to stay at this input frequency during the recording of signals. Identification of resonance is not easy for systems exhibiting non-viscous damping because the maximum amplitude of displacement does not correspond to resonance state. A possible solution lies in recording continuously the phase delay between the applied loading signal and the displacement signal. Another problem arises when the resonance frequency is identified. Due to structure-shaker interaction, the shaker is usually observed to be unable to apply the selected fundamental frequency [28]. In addition, even if the shaker is able to maintain the tested system in a true resonance state, one must ensure that the tested structure is not harmful in such a resonance state which usually induces high amplitudes.

5.3.7 - Acoustics

Ouis [29-31] used the room acoustical technique to detect decay in logs through measuring the dampening of bending vibrations. He presented a technique for evaluating the loss factor of a solid material element, and investigated the example of a Norway Spruce beam like specimen with artificial defects in the form of voids. The reverberation time *RT* is defined as the time in seconds needed for the sound level to drop by 60 dB from the time a sound source has been switched off. Ouis extended this concept to any vibrating system, and evaluated the loss factor η by the relation:

$$\eta = \frac{\ln 10^6}{\omega RT} \approx \frac{2,2}{fRT} \qquad (20)$$

This technique was also employed by Craik and Barry [32].

5.3.8 - Laboratory visco-elastic methods

Mechanical spectroscopy is a popular means for measuring the internal friction of materials. Typically, a torsion pendulum is used to stress harmonically a sample and the lag of the response (strain), relative to the stress, provides the loss tangent and thus the internal friction [33]. In 1984, Wert et al. [34] measured the internal friction and dielectric loss on whole wood, cellulose and lignin to elucidate new features of the loss components. The equipment used for internal friction measurements was a low frequency inverted torsional pendulum which had been designed for use with metals and alloys.

5.3.9 - Correspondence between measurement methods

With the exception of acoustical and visco-elastic methods, the different described methods for evaluating damping are summarized in Table 5.1. In addition, Gade and Herlufsen [35] compared several methods for measuring damping with respect to their advantages and disadvantages and provided a complete correspondence table relating the different quantities provided by different measurement methods.

Table 5.1: Characteristics of selected measurement methods of damping

Method	Time domain	Frequency domain	Impact excitation	Shaker excitation	Measured quantity
Logarithmic decrement	x		x		δ
Envelope fitting	x		x		ξ
Phase plot diagram	x		x		ξ
Half-power bandwidth		x	x	x	η
Resonant amplification		x		x	Q
Experimental modal analysis		x	x	x	ξ
Resonant energy loss per cycle	x			x	ξ,η
Phase angle	x			x	η

The amplification factor Q relates to the hysteretic damping ratio η through the equation:

$$Q = \frac{1}{\eta.\sqrt{1-\eta^2/4}} \approx \frac{1}{\eta} \qquad (21)$$

At resonance, the relationship between hysteretic damping ratio η and (equivalent) viscous damping ratio ξ is:

$$\eta = 2\xi \qquad (22)$$

The viscous damping ratio ξ is obtained from the logarithmic decrement δ as:

$$\xi = \frac{\delta}{2\pi} \qquad (23)$$

Sometimes the specific damping capacity φ is employed, and is defined as:

$$\varphi = 2\pi\eta = 4\pi\xi \qquad (24)$$

5.4 - REFERENCES

1. Ewins, D.J., *Modal testing: theory, practice and application*. 2000, Baldock: Research Studies Press. XIII, 562 s.
2. Maia, et al., *Theoretical and experimental modal analysis*. 1997, Taunton, Somerset, England: Research Studies Press Ltd.
3. Schwarz, B.J. and M.H. Richardson. *Experimental Modal Analysis*. in *CSI Reliability Week*. 1999. Orlando.
4. Reynolds, P. and A. Pavic, *Impulse hammer versus shaker excitation for the modal testing of building floors.* Experimental Techniques, 2000. **24**(3): p. 39-44.
5. Brüel & Kjær. *Product data - Heavy Duty Impact Hammer - Type 8208*. [Accessed 07/02/2011]; Available from: http://www.bksv.com/doc/bp2079.pdf.
6. Smallwood, D.O. and R.G. Coleman, *Force measurements during vibration testing*. 1993: United States.
7. Lindberg, H.E., *Effects of support conditions and shaker arrangements in beam vibration testing.* Planetary and Space Science, 1961. **4**(0): p. 285-300.
8. De Silva, C.W., *Vibration and Shock Handbook*. 2005, Boca Raton: Taylor & Francis. 1872 s.
9. Døssing, O., *Structural testing - Part 1 - Mechanical Mobility Measurements*. 1988, Brüel & Kjær, Denmark.
10. Srikantha Phani, A. and J. Woodhouse, *Viscous damping identification in linear vibration.* Journal of Sound and Vibration, 2007. **303**(3-5): p. 475-500.
11. Srikantha Phani, A. and J. Woodhouse, *Experimental identification of viscous damping in linear vibration.* Journal of Sound and Vibration, 2009. **319**(3-5): p. 832-849.
12. National Instruments. *Modal Analysis*. 2011 [Accessed 31/01/2011]; Available from: http://zone.ni.com/devzone/cda/tut/p/id/8276.
13. Labonnote, N., A. Rønnquist, and K.A. Malo, *Experimental Evaluations of Material Damping in Timber Beams.* Wood Science and Technology, 2012. **(submitted)**.
14. Labonnote, N., A. Rønnquist, and K.A. Malo, *Experimental Evaluation and Semi-analytical Prediction of Material Damping in Timber Panels.* Holzforschung, 2012. **(submitted)**.
15. Labonnote, N., A. Rønnquist, and K.A. Malo, *Prediction of material damping in timber floors, and subsequent evaluation of structural damping.* Engineering structures, 2012. **(to be submitted)**.
16. Clough, R.W. and J. Penzien, *Dynamics of Structures, 2nd edition*. 1993, New York: McGraw-Hill.
17. Fukada, E., *The vibrational properties of wood I.* Journal of the Physical Society of Japan, 1950. **5**: p. 321-327.
18. Obataya, E., T. Ono, and M. Norimoto, *Vibrational properties of wood along the grain.* Journal of Materials Science, 2000. **35**: p. 2993-3001.
19. Maslov, K. and V.K. Kinra, *Damping capacity of carbon foam.* Materials Science and Engineering A, 2004. **367**(1-2): p. 89-95.
20. Gounaris, G.D., E. Antonakakis, and C.A. Papadopoulos, *Hysteretic damping of structures vibrating at resonance: An iterative complex eigensolution method based on damping-stress relation.* Computers & Structures, 2007. **85**(23–24): p. 1858-1868.
21. Cai, Z., et al. *Use of phase-plot to evaluate damping of free vibration in wood-based materials*. 1996: SPIE.
22. Macioce, P., *Viscoelastic damping.* Sound and Vibration, 2003. **37**: p. 8-10.
23. Kavitha, D. and S.R. Damodarasamy, *Basics of Structural Dynamics and Aseismic Design*. 2009, New Delhi: Prentice-Hall Of India Pvt. Ltd.
24. White, M.F. and K.H. Liasjø, *Measurement of mobility and damping of floors.* Journal of Sound and Vibration, 1982. **81**(4): p. 535-547.

25. Nakao, T., T. Okano, and I. Asano, *Theoretical and Experimental Analysis of Flexural Vibration of the Viscoelastic Timoshenko Beam.* Journal of Applied Mechanics, 1985. **52**: p. 728-731.

26. Hwang, S.J., R.F. Gibson, and J. Singh, *Decomposition of coupling effects on damping of laminated composites under flexural vibration.* Composites Science and Technology, 1992. **43**(2): p. 159-169.

27. Amada, S. and R.S. Lakes, *Viscoelastic properties of bamboo.* Journal of Materials Science, 1997. **32**: p. 2693-7.

28. Rønnquist, A., *Pedestrian induced lateral vibrations of slender footbridges*, in *Department of Structural Engineering*. 2005, Norwegian University of Science and Technology: Trondheim.

29. Ouis, D., *Vibrational and acoustical experiments on logs of spruce.* Wood Science and Technology, 1999. **33**(2): p. 151-184.

30. Ouis, D., *Detection of decay in logs through measuring the dampening of bending vibrations by means of a room acoustical technique.* Wood Science and Technology, 2000. **34**(3): p. 221-236.

31. Ouis, D., *An acoustical technique for determining the loss factor of solid materials.* Journal of Testing and Evaluation, 2002. **30**: p. 497-500.

32. Craik, R.J.M. and P.J. Barry, *The internal damping of building materials.* Applied Acoustics, 1992. **35**(2): p. 139-148.

33. De Silva, C.W., *Vibration damping, control and design*. 2007, USA: CRC Press, Taylor & Francis Group.

34. Wert, C.A., M. Weller, and D. Caulfield, *Dynamic loss properties of wood.* Journal of Applied Physics, 1984. **56**(9): p. 2453-2458.

35. Gade, S. and H. Herlufsen, *Digital Filter vs FFT techniques for damping measurements.* Journal of Sound and Vibration, 1990. **24**(3): p. 24-32.

6 - ASSESSMENT OF WALKING-INDUCED FLOOR VIBRATIONS ACCORDING TO THE SBR GUIDELINE

Document written by Sven Lentzen & Arnold Koopman
TNO, Structural Dynamics, Delft

6.1 - Introduction

Lightweight floors are prone to high levels of vibration due to human activities. The Dutch building code imposes regulations on floors with respect to safety, health and serviceability. The walking-induced vibrations of floors are not incorporated in these regulations. The private law arrangement in the NEN 6702 (§10.5.2) [1] does not completely cover the physical background of the issues and is solely applicable to heavyweight floors with two- or four-sided simply supported or clamped conditions. It merely restricts the first eigenfrequency of a floor to be larger than 3Hz for walking and to be larger than 5Hz for jumping. These restrictions are not sufficient for lightweight floors as these are easily excited by the higher harmonics of (near) periodic loads.

Due to the growing interest in lightweight buildings the need for an appropriate assessment guideline for walking-induced floor vibrations increased. From the need of such a guideline two European research projects, funded by the Research Fund for Coal and Steel (RFCS), were initiated to find the appropriate assessment method [3,4]. This resulted into two guidelines, a European [4] and a Dutch one, namely the SBR guideline for walking-induced floor vibrations [5]. The Dutch guideline describes the complete assessment procedure, while the European guideline only covers the so-called hand calculation method.

In the following the general principles of the (Dutch) guideline are described with an emphasis on the experimental method. Finally, some recommendations are made to extend and to improve the guideline.

6.1.1 - Assessment quantity

The guideline introduces a new assessment quantity, namely the OS-RMS_{90} (OneStep-RMS-90). This is the RMS-value of the vibration levels (in mm/s) on a position of the floor during the period of one step. The vibrations not only depend on the floor to be assessed, but they also on the characteristics of the source. The source is determined by the step frequency and the weight of the walking person. The source varies wildly in frequency and load. Therefore, based on a statistical approach, the OS-RMS_{90} describes the vibration level that is not exceeded in 90% of all cases.

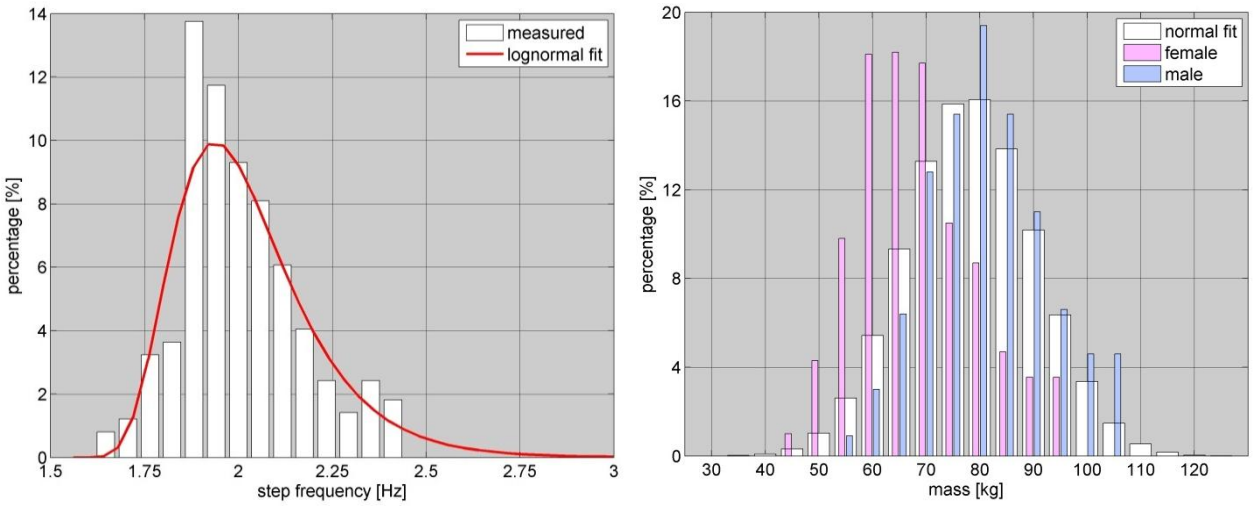

Figure 1: Demographic distribution of step frequencies and weight.

In Figure 1, the demographic distributions of step frequency and weight of the Dutch population is displayed. When the vibration response of the floor to be assessed is obtained for all combinations of step frequency and weight, then the 90%-upper limit of all these combinations (regarding the likelihood of appearance) poses the OS-RMS_{90}.

Due to the modal behavior, the OS-RMS_{90} is very dependent of the locations of excitation and of response. In the guideline it is therefore advised to choose the location of measurement where high nuisance is expected and to choose the location of excitation where walking excitation occurs frequently. In case these locations are unknown it is suggested to choose the floor center as point of excitation and of response.

6.1.2 - Classification

The floor assessment in the SBR-guideline is based on a number of classes. The class 0 – 0.1 is below the threshold of observation. Walking induced vibrations with a OS-RMS_{90} of 0.05 are just noticeable for 50% of the people, but they are not regarded as a annoying. A barely noticeable increase in vibration level occurs when the response increases with a factor 1.4. A clearly noticeable change in vibration level occurs when the response increases with a factor 2. One step in nuisance level is most likely to occur when the response increases with a factor 4. This factor is still under investigation.

These factors define the classes as depicted in Figure 2. For dwellings, the guideline recommends floors of class D (0.8 – 3.2). However, in practice floors in the upper half of this class are regarded as uncomfortable. Therefore, it is suggested by TNO to aim for floors (in dwellings) with an OS-RMS_{90} up to 1.6.

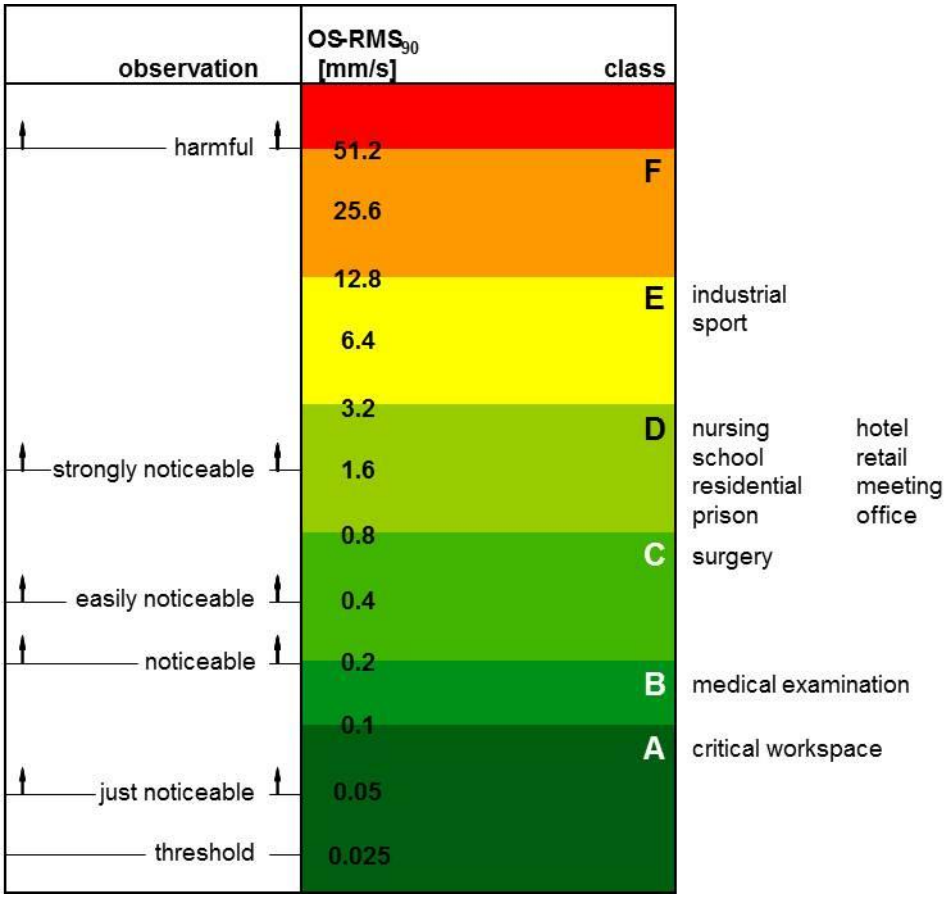

Figure 2: Table with the floor classes according to the SBR-guideline [5]

The guideline is only applicable to the treaded floors. It cannot be used to assess neighboring floors. Vibrations induced outside the sphere of influence are more annoying. Therefore, vibrations induced on neighboring floors have to be assessed more severely than vibrations induced on the floor itself. For this reason the assessment of the neighboring floor can play a more crucial part in the design stage than the treaded floor itself. In order to make the guideline applicable to neighboring floors, the assessment criteria should be altered according to the findings published in the international standard ISO 2631 [6].

According to ISO 2631 vibrations which are just above the threshold of observation can lead to "adverse reactions". Vibrations with the frequency range of 6 to 12Hz (which are common for lightweight floors) are characterized by a threshold of 0.2mm/s (see Figure 3). For the neighboring floor, TNO therefore advises a OS-RMS_{90} < 0.2 (for high comfort: OS-RMS_{90} < 0.1).

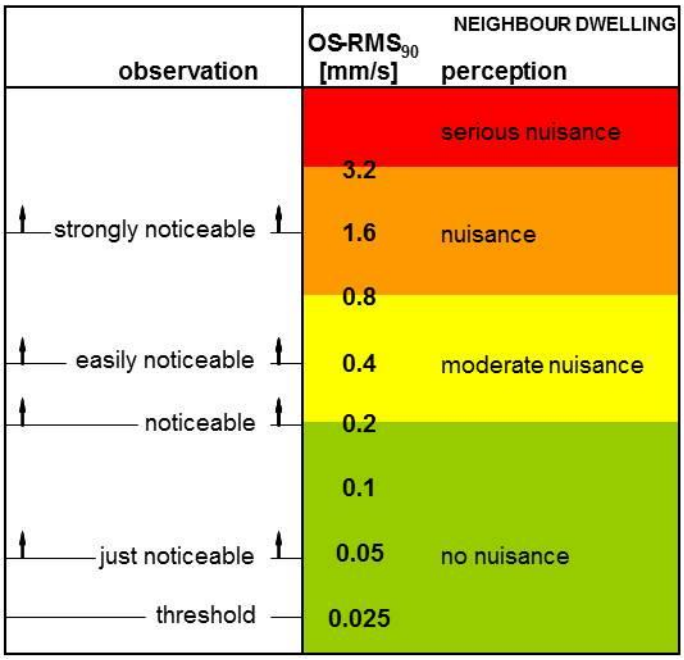

Figure 3: Table with the perception levels at neighboring floors based on ISO 2631 [6]

6.1.3 - Assessment methods

In the Dutch [5] guideline two different methods are presented to determine the OS-RMS_{90}, namely

- the hand calculation method
- the transfer function method

In both methods the walking load is described as a polynomial in time where the coefficients depend on the step frequency and the person's weight [3].

In the hand calculation method each dominant mode is described by a SDOF mass-spring-damper system. When the eigenfrequency, the modal mass and the damping ratio of a dominant mode is known, then the OS-RMS_{90} can be obtained from graphs as shown in Figure 4. Those graphs are presented in the guideline for the damping ratios of 1% to 9%. In case more dominant modes exist then the final OS-RMS_{90} is obtained as the RSS of the OS-RMS_{90} of each individual mode.

The transfer function method is based on obtaining the transfer mobilities from point of excitation to the point of observation and to convolute them with the walking load spectra. The transfer functions can be obtained either numerically (FEM) or experimentally.

In the hand calculation method the eigenfrequency and the modal mass can be obtained using analytical (orthotropic) plate formulation with a predefined set of boundary conditions. The drawback of this method is that neighboring floors cannot be assessed. This drawback is overcome in the transfer function method.

The transfer functions are measured by exciting the floor with the so-called heeldrop-test. At the point of excitation a person between 60kg and 100kg stands on his toes and he subsequentially excites the floor with his heels and waits for six seconds (for highly

damped floors) or sixteen seconds (for low damped floors). This process is repeated 10 times. The forces are measured using force cells, see Figure 5.

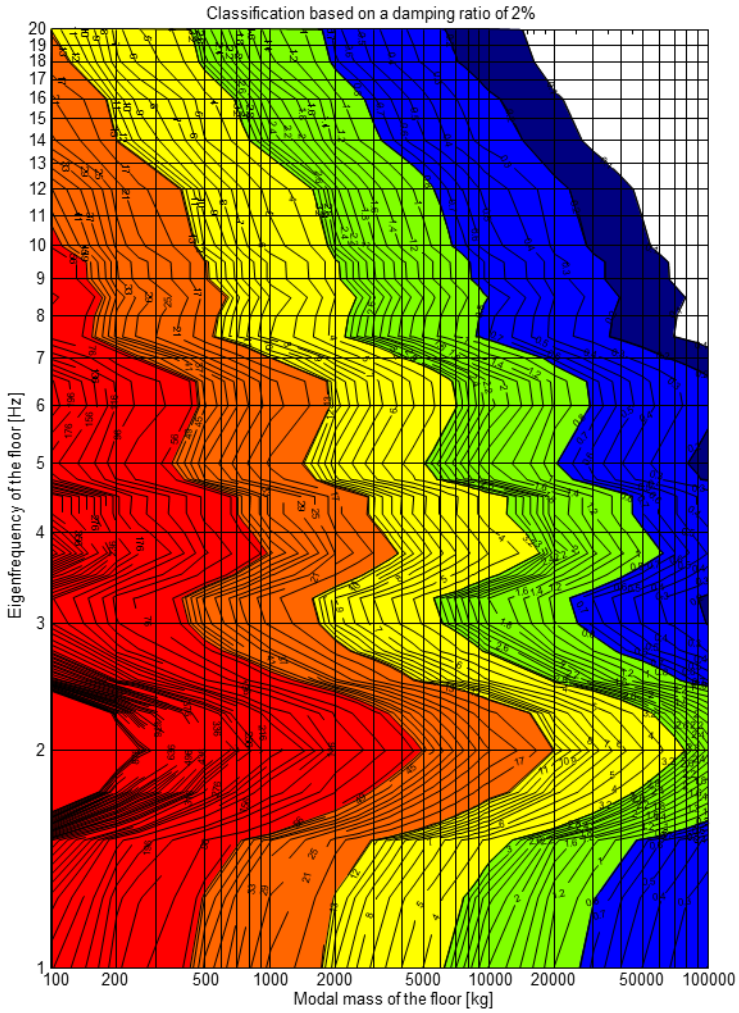

Figure 4: OS-RMS90 isograph for 2% damping

Figure 5: Plateau with force cells to measure the force during a heeldrop-test.

As the accelerations are measured at the points of reception with accelerometers, the transfer mobilities are obtained by integrating the transfer functions between the response and force signals.

6.1.4 - Walking loads

The walking loads are assumed to be described by eighth order polynomials in time

$$F(t) = m(K_1 t + K_2 t^2 + K_3 t^3 + K_4 t^4 + K_5 t^5 + K_6 t^6 + K_7 t^7 + K_8 t^8)$$

Where m is the mass of the walking person and the coefficients K_i depend on the step frequency as described in Table 1.

Table1: Polynom coefficients for the description of the walking load.

	$f_{step} \leq 1.75$Hz	1.75Hz < f_{step} < 2Hz	$f_{step} \geq 2$Hz
K_1	-8 f_{step} + 38	24 f_{step} -18	75 f_{step} -120.4
K_2	376 f_{step} -844	-404 f_{step} +521	-1 720 f_{step} +3 153
K_3	-2 804 f_{step} +6 025	4 224 f_{step} -6 274	17 055 f_{step} -31 936
K_4	6 308 f_{step} -16 573	-29 144 f_{step} +45 468	-94 265 f_{step} +175 710
K_5	1 732 f_{step} +13 619	109 976 f_{step} -175 808	298 940 f_{step} -553 736
K_6	-24 648 f_{step} +16 045	-217 424 f_{step} +353 403	-529 390 f_{step} +977 335
K_7	31 836 f_{step} -33 614	212 776 f_{step} -350 259	481 665 f_{step} -888 037
K_8	-12 948 f_{step} +15 532	-81 572 f_{step} +135 624	-174 265 f_{step} +321 008

In Figure 6 the simulated walking loads for one step and for multiple subsequent steps are displayed.

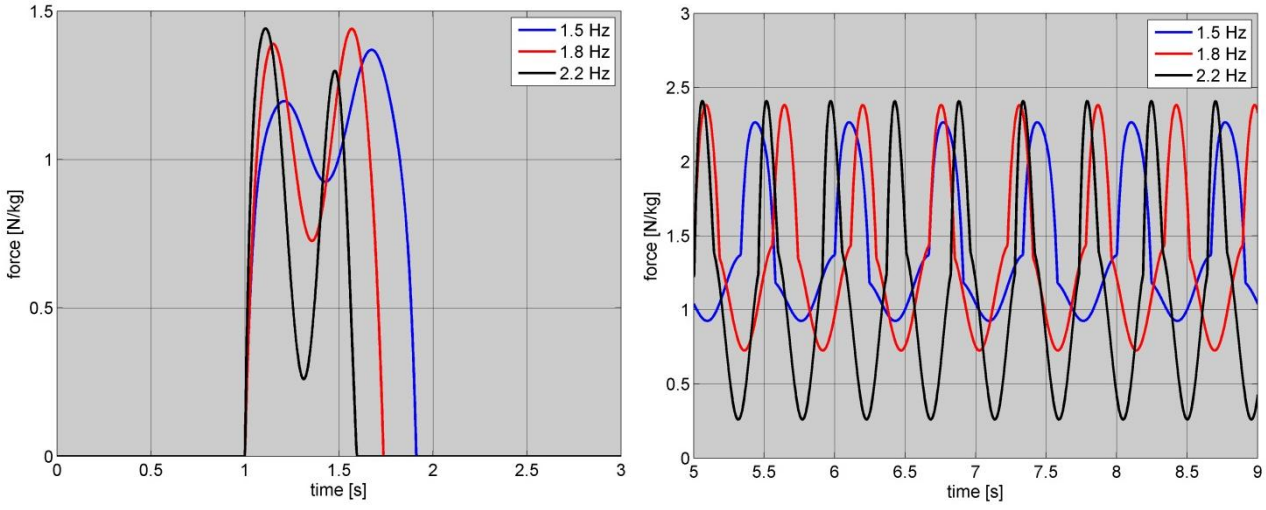

Figure 6: Load trace of a single step (left) and of multiple subsequent steps (right) for three different step frequencies.

The guideline suggests to obtain the walking load spectrum from load time traces which include 50 subsequent steps as depicted by the blue curves in Figure 7.

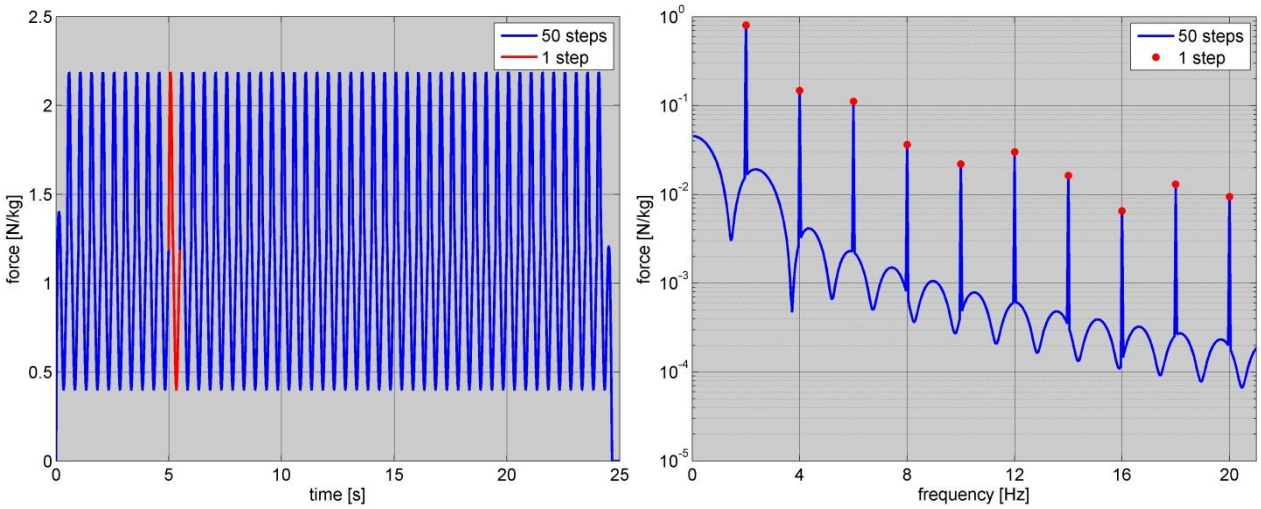

Figure 7: Load trace in the time domain (left) and load trace in the frequency domain (right).

As walking constitutes, according to the guideline, a periodic loading of the floor, it should be sufficient to only obtain the harmonic peaks of the load in the frequency domain. It is therefore also sufficient to only consider a load time trace of length $1/f_{step}$. The resulting load spectrum then only consists of the harmonic amplitudes. This is shown by the red curve and dots in Figure 7.

The response spectrum is obtained by convoluting the load spectrum with the transfer mobilities and the RMS-value during one step is computed as the surface integral of the response spectrum. However, the vibration perception of human beings is frequency dependent and therefore the response spectrum should be weighed before the RMS-value is determined. The weighing function is described according to

$$|H(f)|] = \frac{1}{v_0} \frac{1}{\sqrt{1+\left(\frac{f_0}{f}\right)^2}}$$

where f_0 = 5.6Hz and v_0 = 1mm/s.

6.1.5 - Future recommendations

It has been discussed that the criteria have to be extended to neighboring floors. One could also consider making the guideline suitable to assess the vibrations on balconies or staircases. It is additionally suggested that load spectra should be obtained for the harmonic frequencies.

When the eigenfrequencies and modal ratios are obtained, either analytically or experimentally, then the OS-RMS90 can be determined from several graphs like the one shown in Figure 4. This can be cumbersome especially when values have to be interpolated

between different damping ratios. It is suggested to summarise all graphs into one, as displayed in Figure 8.

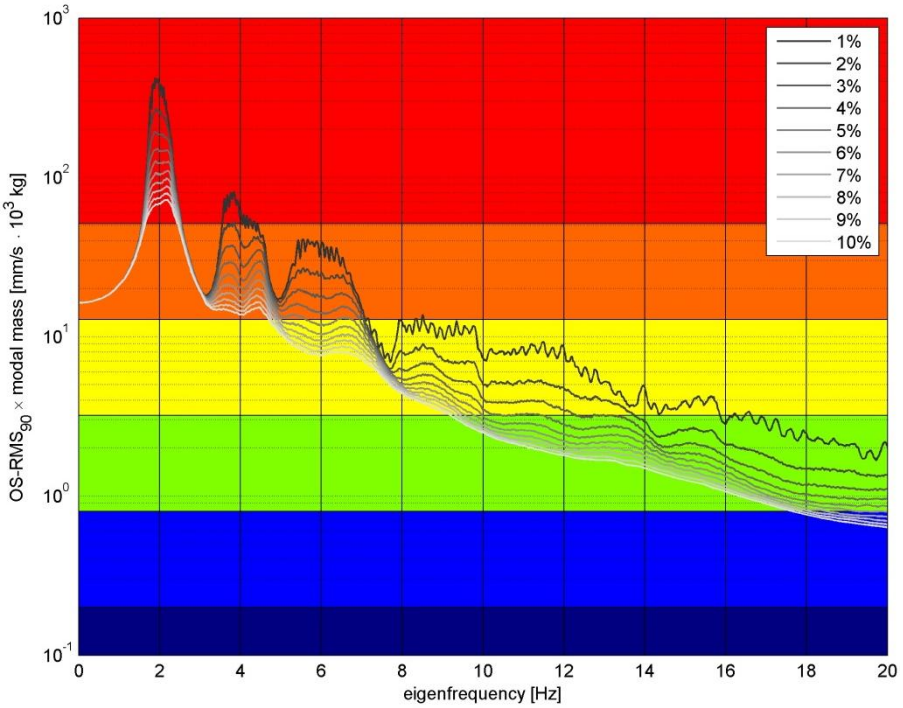

Figure 8: All OS-RMS$_{90}$ iso-graphs summarized into one

From this graph a normalized OS-RMS$_{90}$ value can be determined depending on the eigenfrequency and the damping ratio. Eventually, the normalized value has to be divided by the modal mass in tons.

For the sake of reproducibility of the measurements it is recommended to not perform the assessment based on the maximum vibration level, but rather the 50, or 90-percent upper level over the floor.

The assessment described in the guideline is based on the assumption that a stationary state of vibration can be reached. For small floor, such as balconies, this is rarely the case. Also, the guideline assumes perfect symmetrical striding. In practice this is rarely occurs, which results in an overestimation of the higher harmonics of the load spectrum. Therefore, in the literature a distinction is made between LFF (low-frequencies floors) and HFF (high-frequency floors). Stationary behavior is to be expected in LFF, which have a first eigenfrequency below around 10Hz and can thus resonate with the lower harmonics. Transient response is to be expected with HFF as the higher harmonics are in general to be neglected. It is therefore recommended to extend the guideline to assess the transient behavior of floors due to walking.

6.2 - References

[1] NEN 6702, Technische grondslagen voor bouwconstructies – TGB 1990 – Belastingen en vervormingen, 2007.

[2] M. Feldmann, C. Heinemeyer, E. Caetano, A. Cunha, F. Galanti, A. Goldack, O. Hechler, S. Hicks, A. Keil, M. Lukic, R. Obiala, M. Schlaich, A. Smith, P. Waarts, Human induced Vibration of Steel Structures - HIVOSS: Design Guideline and Background Report, Technical Report RFCS, EUR 24183 EN, European Commission, 2010.

[3] G. Sedlacek, C. Heinemeyer, C. Butz, B. Völling, P. Waarts, F. van Duin, S. Hicks, P. Devine, T. Demarco, Generalisation of criteria for floor vibrations for industrial, office, residential and public building and gymnastic halls, Technical Report RFCS, EUR 21972 EN, European Commission, 2006.

[4] HIVOSS, Vibration Design of Floors, Guideline RFS2-CT-2007-00033, Technical Report, RFCS, 2007.

[5] SBR richtlijn – Trillingen van vloeren door lopen. Richtlijn voor het voorspellen, meten en beoordelen, 2005.

[6] ISO 2631-2:2003, Mechanical vibration and shock – Evaluation of human exposure to wholebody vibration – Part 2: Vibration in buildings (1 Hz to 80 Hz), ISO, Geneva, Switzerland, 2003.